



TEKNOFEST
AVIATION, SPACE AND TECHNOLOGY FESTIVAL

FIGHTER UAV COMPETITION 2022

CRITICAL DESIGN REPORT

TEAM NAME: AL-BURAQ
AUTHORS: All Team Members

Contents

1 BASE SYSTEM SUMMARY	1
1.1 System Description	1
1.2 System Final Performance Specifications	1
2 ORGANIZATION SUMMARY	3
2.1 Team Organization	3
2.2 Timeline and Estimated Budget	4
2.2.1 Schedule timeline	4
2.2.2 Budget Planning	4
3 DETAILED DESIGN SUMMARY	6
3.1 Final System Architecture	6
3.1.1 System Architecture	6
3.1.2 Components selection	7
3.2 Subsystems Summary	12
3.3 Aircraft Performance Summary	12
3.4 3D Design of Aircraft	17
3.5 Aircraft Weight Distribution	19
4 AUTONOMOUS MISSIONS	20
4.1 Autonomous Lockdown	21
4.2 Kamikaze Mission	26
5 GROUND STATION AND COMMUNICATION	29
6 USER INTERFACE DESIGN	35
7 AIRCRAFT INTEGRATION	38
7.1 Structural Integration	38
7.2 Mechanical Integration	40
7.3 Electronic Integration	41
8 TEST AND SIMULATION	43
8.1 Sub-System Tests	43
8.2 Flight Test and Flight Checklist	49
9 SAFETY	50
References	51

1 BASE SYSTEM SUMMARY

1.1 System Description

Within the scope of the Fighting UAV competition, autonomous take-off, flight, landing, locking and real-time video and telemetry data stream tasks were examined and a general system architecture was constructed. In this setup, a system that can fulfill the tasks has been established, this system has been designed to meet the requirements, literature research has been done, it has been conceptually designed, produced and sub-tested.

With high power GPU based ground station and processor for high frequency decision making and communication between multi-nodes of competition server, on-board system. High speed multi-core on-board processing unit to control vehicle attitude and tracking in dog-fight mode and lock in kamikaze mission. Server API node is designed to communicate with the server competition. beside a message broker to communicate between internal nodes and on-board companion computers, a multi-channel high power RF telemetry communication module to communicate with both flight controller and companion computer in real-time and with antennas covering a high range of angles to ensure communication in any vehicle's orientation during maneuvers. Also independent FPV real-time video stream with two good fitting antennas to ensure high rate high resolution video stream all flight time.

System software and control algorithms conceptually designed, simulated and sub-tested to fit with our UAV and communication chart. Communication diagram, system architecture, mechanical design, aerodynamic system, and control algorithms and software is discussed in detail in following sections.

Al-Buraq UAV with simple yet effective aerodynamics to achieve the required task. Such as, low aspect ratio for higher maneuverability, back swept wing to allow high speeds, raked wingtip to avoid the wingtip vortices, semi symmetric airfoil to get advantage of lift and maneuverability. Moreover, relying on a battery powered motor with a high pitch pusher propeller to ensure high thrust to weight ratio.

1.2 System Final Performance Specifications

Cruise speed	35 m/s
Rate of climb	8 m/s
C_d	0.064
C_l/C_d	40
Thrust / weight	1

Table 1 continued from previous page

Cruise speed	35 m/s
Stall speed	12 m/s
Max speed at 0 AoA	45 m/s
Max AoA	12°
Max bank angle	60°
Max rate of decent	8 m/s
Flight time	27 minute
Take off weight	5270 gr

Table 1: System Final Performance Specifications

These results proved that the vehicle is well suited for the required task:

- A low drag value resulting in low power consumption and long endurance.
- A wide range of speed offering good handling for both low and high speed scenarios.
- A high maneuverability due to sufficient climbing rate and wide angle of movement on three axis (pitch, yaw and roll)

With the outstanding aerodynamic and propulsion performance that optimized for the task of dog and kamikaze fight missions, Flight controller system of Pixhawk cube and companion computer to ensure high rate attitude-velocity control of the vehicle during autonomous flights and missions along side good ground station relays on powerful gpu for video processing and decision making; software system of filters, estimation algorithms, detection AI models, decision making algorithms, between nodes message broker, competition server API, and position-attitude controllers well designed to have high speed high resolution smooth behavior of the vehicle during the required missions. Outer control and prediction loop of frequency of 25 HZ with internal attitude control loop of 400HZ, detection and video stream of 30 FPS, with high rate and bandwidth communication channels; Our flight system can achieve good tracking performance with tuned controller and limit coefficients.

2 ORGANIZATION SUMMARY

2.1 Team Organization

Salah Gallo (Team Leader)		Yasin Arslan (Advisor)	
Mechanical Team	Albara Mohamed (Team Leader)	Omar Abdelmoaty	Abdelbasset Sedjai
Software Team	Ahmed ElGreetly (Team Leader)	Youssef Darahem	Anas Badawi
Control Team	Halid Biltaci (Team Leader)	Moustafa Hassanein	Ahmed Elsheikh

Table 2: Team Structure

Sallah Gallo – Team Leader, B.Sc. Electrical and Electronics Engineering, Istanbul University, MBA

Yasin Arslan – Advisor, Istanbul Technical University, PhD. Mechanical Engineering

Mechanical Team:

Description: The Designing and the manufacturing of the UAV body, wings and mechanisms.

Team Members:

- Baraa Tawakol, İstanbul Technical University, M.Sc. Aeronautics and Astronautics Engineering
- Omar Abdelmoaty, Bilgi university, B.Sc. Mechatronics Engineering
- Abdelbasset Sedjai,

Software Team:

Description: Implementation of the detection algorithms, communication between the UAV and ground station, and between ground station and competition server.

Team Members:

- Ahmed Elgreetly, Near East University, B.Sc. Electrical and Electronics Engineering
- Youssef Darahem, Medipol University, B.Sc. Computer Engineering
- Anas Badawi, Bilgi university, B.Sc. Computer Engineering

Control Team:

Description: Flight controller configuration, components and power system integration, and mission and tracking motion control.

Team Members:

- Halid Biltacı, İstanbul Technical University, M.Sc. Aeronautics and Astronautics Engineering
- Moustafa Hassanein, İstanbul Technical University, B.Sc. Control and Automation Engineering
- Ahmed Elsheikh, Medipol University, B.Sc. Electrical and Electronics Engineering

2.2 Timeline and Estimated Budget

2.2.1 Schedule timeline



Figure 1: Schedule timeline

2.2.2 Budget Planning

Component Name	Price (\$)	QTY	Total Price	Department
5mm*5mm basla	4,5	10	45	Mechanical
4mm yuvarlak balsa	7,5	20	150	Mechanical

Table 3 continued from previous page

Component Name	Price (\$)	QTY	Total Price	Department
push rod steel	6,25	4	25	Mechanical
landing gear anti vibrations	11	2	22	Mechanical
shrink film kaplama	13	10	130	Mechanical
1mm basla	4,75	40	190	Mechanical
Servo Connectors	1,6	10	16	Mechanical
8*6 mm carbon fiber	2,25	20	45	Mechanical
12mm aluminuum	2,5	6	15	Mechanical
menteşe	0,5	64	32	Mechanical
motor 720kv	82,5	2	165	Mechanical
props	7,5	10	75	Mechanical
retract landing gear	62,5	2	125	Mechanical
landing gear	27,5	2	55	Mechanical
servo motors	11,5	8	92	Mechanical
ıslı Shrink Film iron	60	1	60	Mechanical
epoksi	52,5	2	105	Mechanical
carbon fiber kumas	300	1	300	Mechanical
ESCs	43,33	6	259,98	Mechanical
battery	135	2	270	Mechanical
carbon fiber 10*8	7,5	4	30	Mechanical
glass fiber	370	1	370	Mechanical
3mm balsa	180	1	180	Mechanical
carbon fiber 6*4	10	10	100	Mechanical
cam fiber 4mm	3,6	10	36	Mechanical
standard pix tele	75	1	75	Electrical & Control
Remote control	460	1	460	Electrical & Control
pix cube	400	1	400	Electrical & Control
HERE GPS	190	1	190	Electrical & Control
RC transmitter module	50	1	50	Electrical & Control
RC reciever	50	1	50	Electrical & Control
Herelink	1000	1	1000	Electrical & Control
servo for AT	5	1	5	Electrical & Control
Battery charger	150	1	150	Electrical & Control
air pressure sensor	80	1	80	Electrical & Control
rocket dish antenna	160	1	160	Electrical & Control
UBEC (5V 5A)	4	5	20	Electrical & Control
HDMI action camera	80	1	80	Electrical & Control

Table 3 continued from previous page

Component Name	Price (\$)	QTY	Total Price	Department
Telemetry	285	1	285	Electrical & Control
CSI HQ camera	100	1	100	Electrical & Control
		Total	\$5.997,98	

Table 3: Budget Planning

3 DETAILED DESIGN SUMMARY

3.1 Final System Architecture

3.1.1 System Architecture

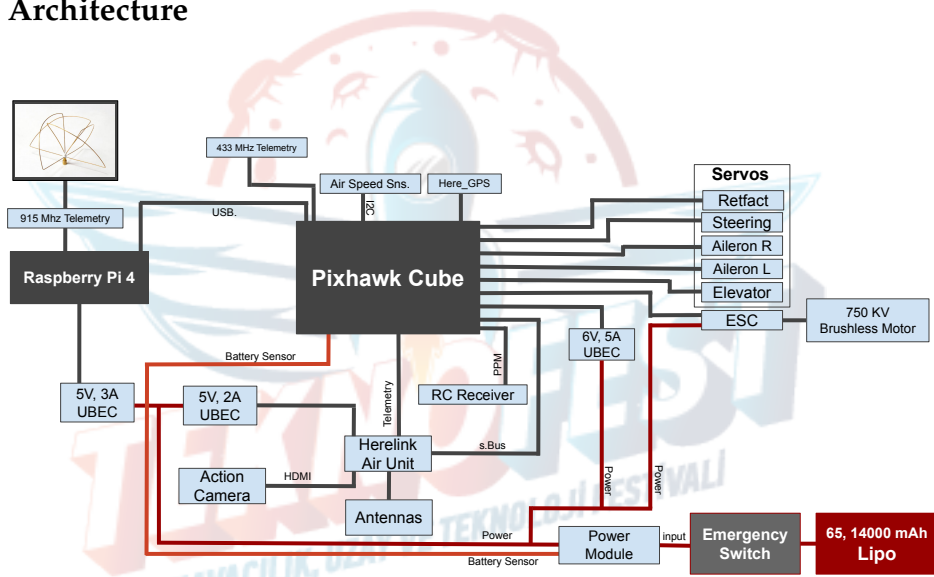


Figure 2: Architecture of the on plane system

- Companion computer is responsible for the task of controlling the flight controller attitude in dog-fight mode and kamikaze fight mode, location estimation and tracking of enemies in both fight-dog and search mode. Companion computer is not responsible for detection; it's only for position and tracking prediction and attitude control. Companion computer used instead of direct ground station control for high frequency estimation and control.
- HereLink is the video transmission channel with the ground station; it's used for its good full-deblieux two antennas to ensure coverage in all orientations of the vehicle with high frequency rate of 30fps.

- GoPro Hero 4 camera with hdmi live output for damped focused high frequency frames with the high speed motion and accelerations of the vehicle.
- Power module and emergency switch for safety and to monitor the current and voltage of the battery.
- UBEC and BEC used to regulate voltage with enough current for all components.

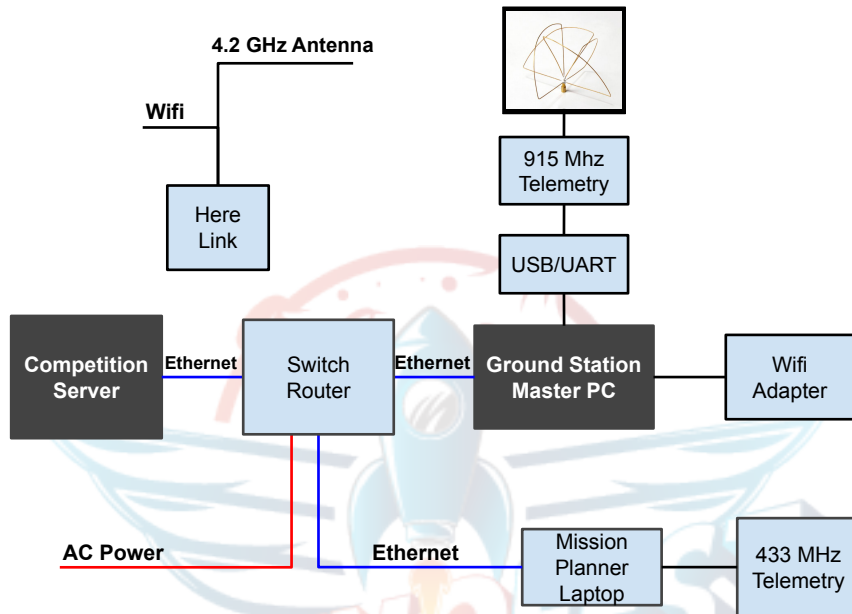


Figure 3: Architecture of the ground station system

- The PC computer is the master unit in the system; it's responsible for communicating with the competition server ,flight controller and on-board companion computer. It's designed to maintain communication, decision making and mode change, video processing and object detection AI models.
- Ground station consists of the main unit (Powerful PC) and laptop for the mission planner interface as second channel for monitor and control. Communicate with flight controller and camera stream through Here-Link, and with on-board computer with the 915Mhz RF module.

3.1.2 Components selection

- **Motor:**

- Lightweight X3520-520kv Sunnysky motor that supports enough thrust for acrobatic, 3D flying, maneuvering, diving, and recovering.

- **Servo Motors:**

- High resolution and high torque RC Servo Motors that have digital metal gear to ensure smooth movement of the control surface (ailerons, elevator, and rudder), which provides stable and safe flight.

- **Electronic Speed Control(ESC):**

- 80A ESC that has a Battery Eliminator Circuit (BEC). This feature ensures that a second set of RC batteries is not required to power the RC receiver and RC servos. This feature obviously saves weight and makes for a safer installation.

- **Battery :**

- lightweight 6s 14000mAh LiPo battery serves as the main power source for the on-plane system and actuators. With a high discharge rate of 25C to be able to provide the required current.

- **90A Power module:**

- As a sensor for having feedback measurements from the battery it simply takes the current and voltage and connects to the controller to make monitoring the energy dissipated in the system power module an advantage for keeping the UAV safe and protecting the system from short circuits.

- **Pixhawk flight controller:**

- Pixhawk Cube Flight controller unit with multi high resolution IMUs and CPU; provides smooth flying. An open-source flight controller gives us the privilege of editing and adding new features to the code with a lot of available libraries to be used, with support for multiple sensors, actuators, and communication modules.

Cube Orange Features:

- Faster H7 SOC with 1MB ram
- Upgraded triple redundant IMU sensors for extra redundancy
- 2 sets of IMU are vibration-isolated mechanically, reducing the effect of frame vibration to state estimation
- IMUs are temperature-controlled by onboard heating resistors, allowing optimum working temperature of IMUs

- The entire flight management unit(FMU) and inertial management unit(IMU) are housed in a relatively small form factor (a cube).
- Fully Cubepilot carrierboard compatible, all inputs and outputs go through a 80-pin DF17 connector, allowing a plug-in solution for manufacturers of commercial systems. Manufacturers can design their own carrier boards to suit their specific needs now and in the future.

Specifications:

• Processor:

- 32bit ARM@ STM32H753 Cortex(R)-M7 (with DP-FPU)
- 400 Mhz/1 MB RAM/2 MB Flash
- 32 bit STM32F103 failsafe co-processor

• Sensors:

- Three redundant IMUs (Accelerometers/Gyrosopes), Two Barometers, One Magnetometer
- ICM 20649 integrated accelerometer / gyro, MS5611 barometer on baseboard
- InvenSense ICM20602 IMU,ICM20948 IMU/MAG, MS5611 barometer on temperature controlled, vibration isolated board
- All sensors connected via SPI

• Power:

- Redundant power supply with automatic failover
- Servo rail high-power (7 V) and high-current ready
- All peripheral outputs over-current protected, all inputs ESD protected

• Interfaces:

- 14x PWM servo outputs (8 from IO, 6 from FMU)
- S.Bus servo output
- R/C inputs for CPPM, Spektrum / DSM and S.Bus
- Analogue / PWM RSSI input
- 5x general purpose serial ports, 2 with full flow control
- 2x I2C ports

- SPI port (un-buffered, for short cables only not recommended for use)
- 2x CAN Bus interface
- 3x Analogue inputs (3.3V and 6.6V)
- High-powered piezo buzzer driver (on expansion board)
- High-power RGB LED (I2C driver compatible connected externally only)
- Safety switch / LED
- Optional carrier board for Intel Edison (now obsolete)

- **Radio controller:**

- Frsky Taranis X9 9-channel radio controller joystick for controlling the UAV in manual mode and switching between different modes, with a high range R9M module.

- **Ground control station:**

- As the Ground Control Station is based on Mission Planner software, a full featured and open source platform it allows multi mode command, safe communication link and high aspect integration. Beside the powerful master ground control station PC which helps in detection and communication with competition servers. PC with high GPU power and CUDA cores will be used to preform this task.

- **HERE+ GPS:**

- Here+ GPS kit is for having an accurate position estimation compared to the normal one because it uses centimeter-accurate ranging with millisecond latencies system which enables high precision flight and safe take-off and landing.

- **Airspeed pressure sensor:**

- The airspeed pressure sensor is for measuring the true airspeed, which enables the UAV of more precise control.

- **Ground station:**

- Powerful PC with high GPU power to communicate with all nodes and detection on live feed.

- **Raspberry pi 4:**

- Raspberry pi is low power consumption and provides good processing speed for our task, and has multiple I/O pins and ports that could be used to control multi-sensors, with the USB3 port enabling high-speed.
- **GoPro Hero 4:**
 - Forward visual camera to track and detect the targets; action camera for high resolution and high FPS with auto-focusing and damping in high speed motion and acceleration on air due the maneuvers. Also support HDMI live output to be passed to Here-link to ground station.
- **HereLink:**
 - A video feed and telemetry channel between the flight controller and forward camera, and the ground station computer high speed and high range. With high speed video processing and API for RTSP video stream and telemetry data, HereLink provides a high rate stream of 30 FPS and high range of 20 Km, high transmitted power and receiving sensitivity with circular polarized antenna and two patch antennas that ensure coverage in any orientation during flight.
- **433Mhz telemetry:**
 - 433MHz is used as a redundant telemetry channel to ground stations with 1W transmission power for high range. It is used for safety to monitor and control the vehicle from a laptop as a second channel in case of system failure.
- **915MHz telemetry:**
 - 915MHz is used with a circular polarized antenna to ensure coverage during vehicle's maneuvers, with 500mW transmission power for high range. This channel used to communicate between the ground station and companion computer to send modes, enemy's locations and detection resulting in dog-fight mode.
- **90A emergency switch:**
 - A box for high current 80A fuse to protect the short circuit and fit with the power consumption of the system. Safety switch with XT60 Cable to be easy to pull and cut power in case of emergency.

3.2 Subsystems Summary

Communication architecture in Figure 17 , had changes to ensure coverage data stream during all orientations and maneuvers of the vehicle and high data rate. This architecture is based on the software architecture where the video processing and detection is on the ground station PC, and attitude controller on board.

The architecture is considering the minimization of the body size and weight of the on-board components for minimization of the stall speed and drag.

processing is divided into two units;

- on-board processing prediction and estimation of the position of the enemy in global coordinate and image frame, vehicle's location and attitudes. Beside the attitude PID controller with the position attitude and enemy's position in frame errors. This processing needs to be done on-board to ensure high frequency rate of prediction and control with callback attributes for the EKF flight controller data.
- PC ground station for decision making ,AI detection models and communication with all nodes.

Video stream with a high rate of 30 fps and delay of 150 ms is fitting the rate of the object detector model on the pc.

For the small delay of video stream and possible rate of detection less than 20 fps, an on board system contains predictions using measurements of both enemy's location and detection result to compensate for that delay to ensure real-time.

On-board computer with high frequency and multi-core processors is used for the high rate attitude control of the vehicle during the fight mission, and position tracking during search and track mode.

3.3 Aircraft Performance Summary

To ensure a long endurance for the vehicle the body was built with lightweight material, the body structure weight is only 800gr. The total take-off weight with payload installed is 5270gr. The task requested from the vehicle requires a high capability of maneuver and good climbing rate, thence the motor chosen to provide thrust is capable of delivering a thrust to weight ratio equal to 1. the climb rate can reach a max of : 8 m/s The slender and clean body design generates a small force of the drag, the wing tips are also equipped with a steam line device that helps to reduce wingtip vortices and decrease their overall effect on the drag. based on simulations and numeric calculation to lift to drag ratio $C_l/C_d = 40$

The stall speed is calculated according to the following equation:

$$v = \sqrt{\frac{2 \times W}{\rho \cdot C_d \cdot S}} = 12.5 \text{ m/s} \quad (1)$$

Following real life testing the stall speed was measured at 12 m/s

Other aspects of flight performance were calculated to evaluate the maneuver capability of the aircraft.

The max speed at zero angle of attack:

$$v = \sqrt{\frac{2 \times T_{max}}{\rho \cdot C_d \cdot S}} = 45 \text{ m/s} \quad (2)$$

The max tested bank angle: 60° degree Radius of turn:

$$r = \frac{\text{speed}^2}{g \cdot \tan(\text{bank}_{\text{angle}})} \quad (3)$$

minimum radius of turn is 13 m, to make one turn in 6 seconds.

Max rate of descent:

$$\frac{W \cdot \sin(\text{angle} - \text{descent}) \cdot V - D \cdot V}{W} = 8 \text{ m/s} \quad (4)$$

The following figure demonstrates a plot of thrust vs efficiency in correlation with voltage levels.

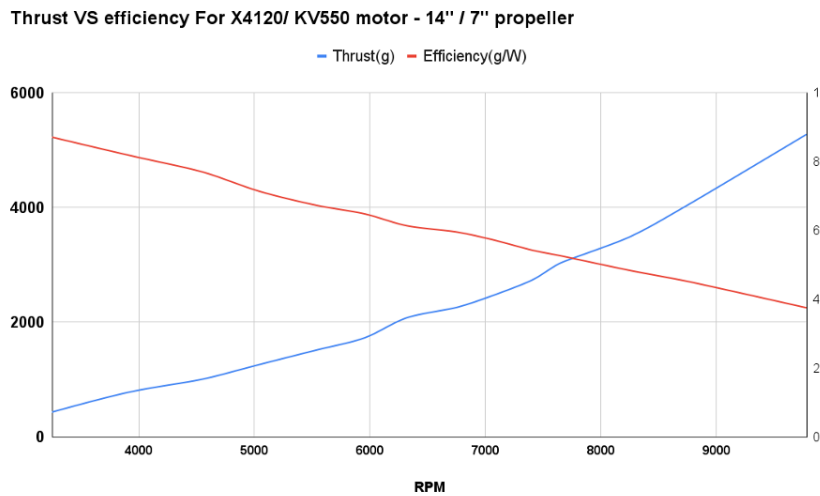


Figure 4: Thrust VS efficiency For X4120/ KV550 motor 14" / 7" propeller

The cruise speed is calculated based on the highest speed acquired at the lowest power consumption while considering drag force.

The optimal efficiency point for the designated motor is at 7411 rpm.
cruise speed of 35 m/s:

$$v = \sqrt{\frac{2 \times T_{maxPerformance}}{\rho \cdot C_d \cdot S}} = 35m/s \quad (5)$$

Voltage(V)	Amps (A)	Thrust(g)	Watts (W)	Efficiency(g/W)	RPM
22.51	2.2	432	49.61	8.71	3248
22.49	4.21	776	94.7	8.19	3906
22.47	5.84	1010	131.2	7.69	4560
22.43	7.86	1260	176.32	7.14	5040
22.35	10.06	1514	224.77	6.73	5537
22.31	11.95	1728	266.69	6.48	5955
22.24	15.18	2073	337.53	6.14	6313
22.18	17.13	2261	379.89	5.95	6758
22.16	19.27	2455	427.08	5.74	7050
22.09	22.87	2742	505.1	5.42	7411
22.02	26.05	3023	573.64	5.27	7640
21.86	33.07	3498	722.82	4.83	8260
21.69	41.19	4041	893.32	4.52	8748
21.19	66.31	5277	1405.08	3.75	9780

Table 4: Motor test report for 6s battery and 14x7 propeller

Flight time:

Used battery is 14000mAh 6s battery. Power of 320 Wh power capacity. 505 watt motor power consumption for cruise and maximum used during take-off and high rate of climb times of 1400 watt averaging 650 watt consumption of motor. 5 V: 2.5A average consumption of on-board processing units + 3A average servos consumption + 1 A for herelink unit + 1 A for other telemetries; totaling around 40 watt system consumption.

$$\frac{320W \text{ battery power}}{\text{Average total power consumption of } 700W} \times 60 = 27.5\text{minutes} \quad (6)$$

of flight at most power consumption scenarios. which is 35% more than needed for round time as a factor of safety.

Reynolds number calculator

Velocity	<input type="text" value="20"/>	m/s	44.739 mph	72 kph
Chord width	<input type="text" value="0.28"/>	m	0.91864 ft	11.024 in
Kinematic Viscosity	<input type="text" value="1.4207E-5"/>	m ² /s	1.529e-4 ft ² /s	
Reynolds Number	394,172			
<input type="button" value="Calculate"/>				

Reynolds number calculation

The Reynolds number is a dimensionless value that measures the ratio of inertial forces to viscous forces and describes the degree of laminar or turbulent flow. Systems that operate at the same Reynolds number will have the same flow characteristics even if the fluid, speed and characteristic lengths vary.

The Reynolds number is calculated from:

$$Re = \frac{\rho v l}{\mu} = \frac{v l}{\nu}$$

Where:

v = Velocity of the fluid

l = The characteristics length, the chord width of an airfoil

ρ = The density of the fluid

μ = The dynamic viscosity of the fluid

ν = The kinematic viscosity of the fluid

Figure 5: Reynold number calculator

The following plot demonstrates the performance of the airfoil chosen for the main wing. Each figure shows the data for two different Reynolds numbers: 250 000 and 500 000 respectively. The plot shows the good performance in a wide range of AoA while giving a good lift performance in correlation to the drag force.

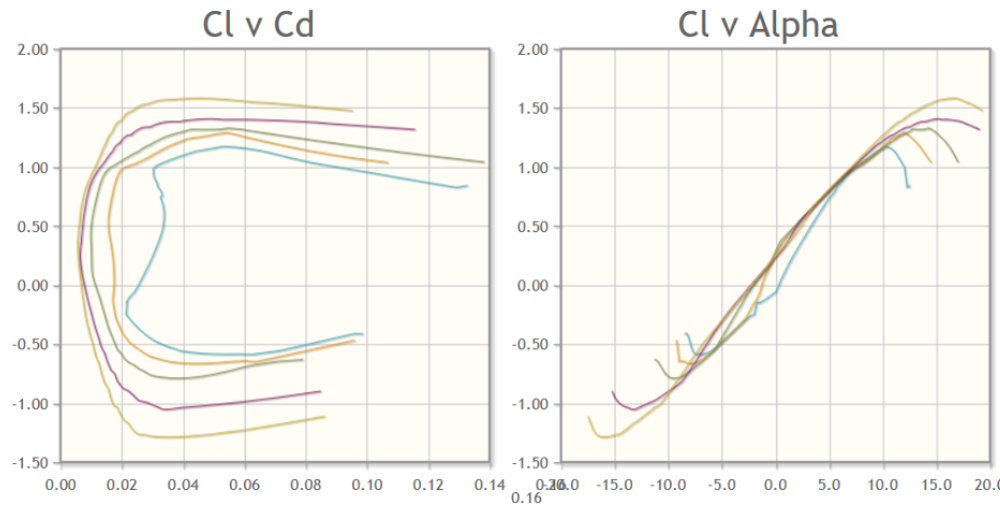


Figure 6: airfoil NASA's data

A simulated calculation was performed to define the drag amount of each major component of the vehicle on OpenVSP alongside Ansys Fluent CFD simulations. The simulation was run based on the following conditions:

- Air speed: 20 m/s
- Temperature: 25°C
- Altitude: 100 m AGL

Component Name	$S_{wet}(cm^2)$	$L_{ref}(cm)$	t/c or d/l	Reynold number	$f(cm^2)$	Cd	% Total
Wing	9417.27	26.79	0.11	314328.6	65.84	0.0142	22.31
Camera	162	3	0.41	35197.39	160.14	0.0347	54.27
Fuselage	4815.26	146	11.76	1712964	20.31	0.0044	6.88
Tail	3096.95	22.99	0.09	269820.3	21.58	0.0046	7.31
Rudder	755.09	13.61	0.09	159742	5.87	0.0012	1.99
Motor support	118.09	5	0.88	58662.31	12.27	0.0026	4.16
Motor	122.74	8.85	1.79	103863.8	2.47	0.0005	0.83
Propeller	114.20	2.11	0.5	24760.72	6.55	0.0014	2.22
Totals:					295.07	0.0640	100

Table 5: Coefficients of drag

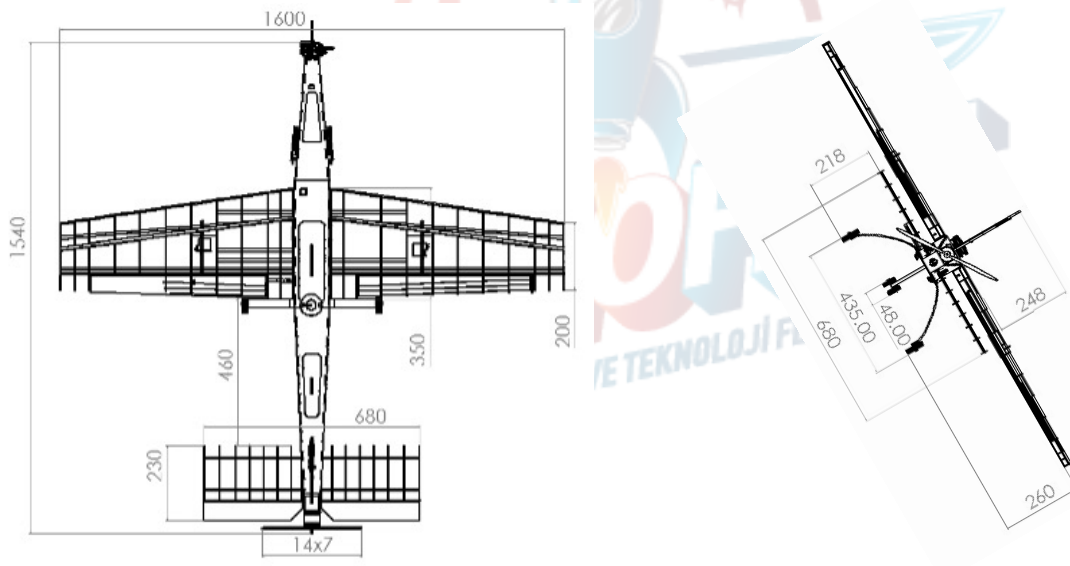
Conclusions made of this simulation and output that surface like camera result in high Cd value, so all surface is flitted and minimize all perpendicular areas.

3.4 3D Design of Aircraft

Using the CAD program we were able to create the 3D model of our UAV. And designing all the parts with the real dimensions and weights which helped us to choose the suitable fuselage area and to distribute the components based on its weight.



Figure 7: 3D Design



(a) Top

(b) Back

Figure 8: 2D Drawings

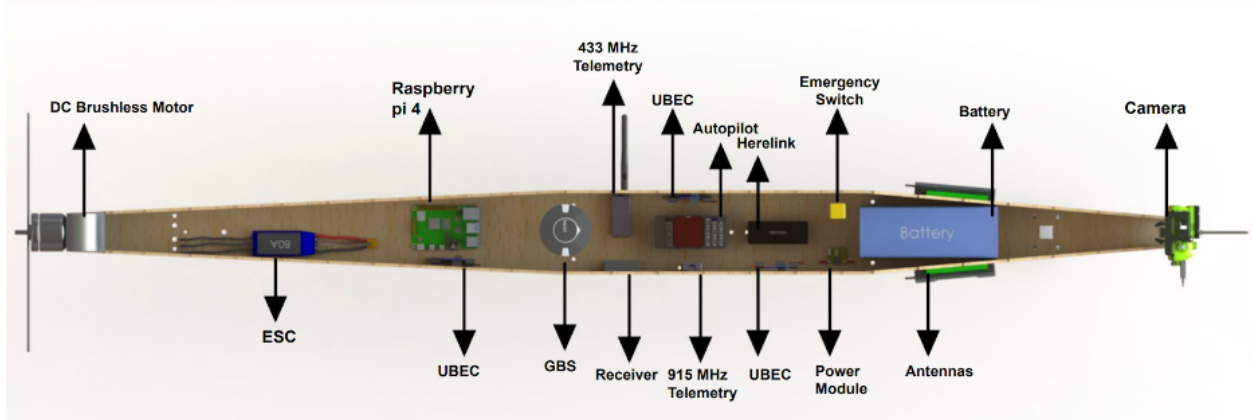


Figure 9: Fuselage internals



Figure 10: Prototype 1

3.5 Aircraft Weight Distribution

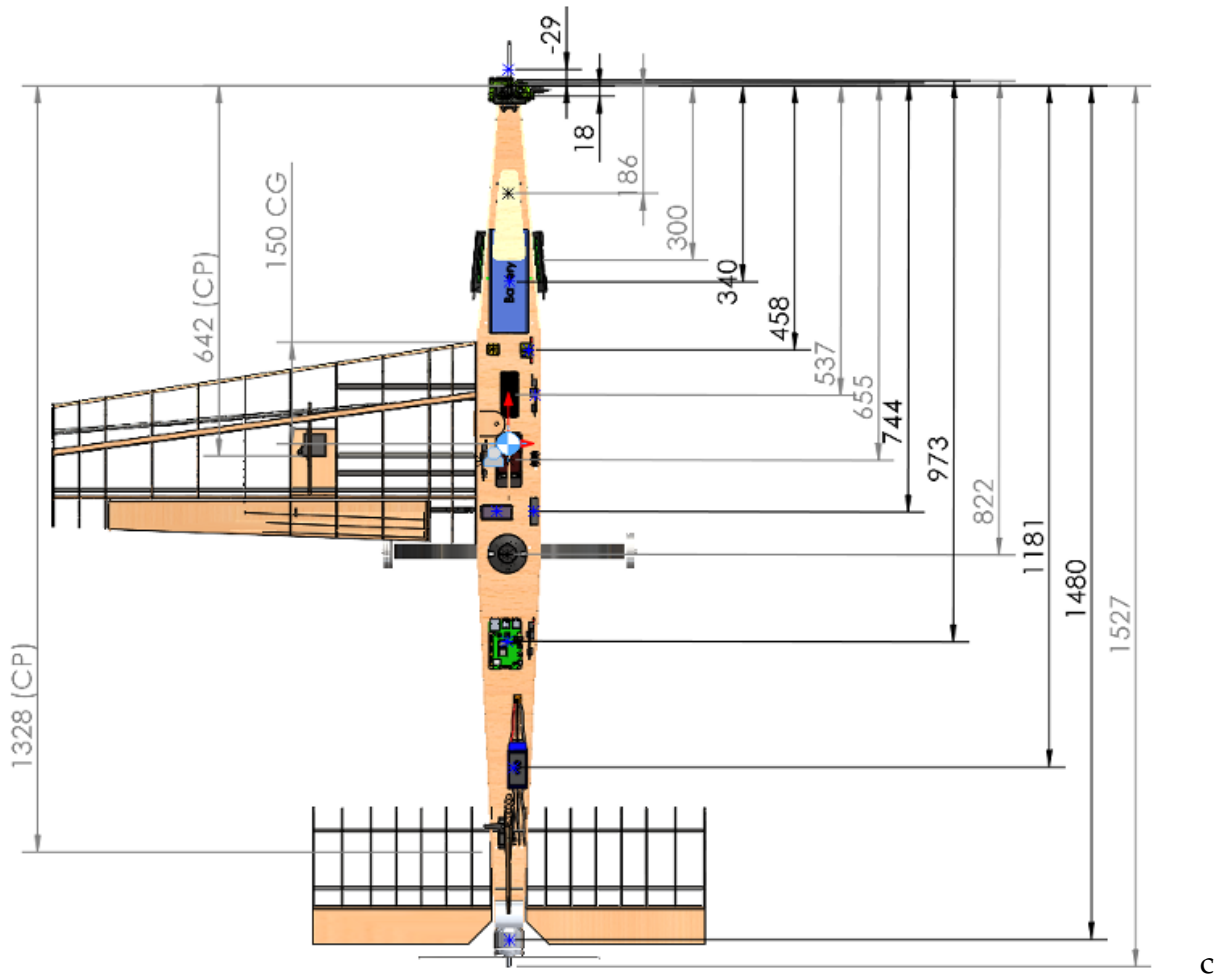


Figure 11: Fuselage Component Distribution

Component	weight (gram)	distance from nose (mm)
Airspeed sensor	20	-29
Camera & housing	150	18
Nose landing gear	200	86
Antennas x2	50	300
Battery	2000	340
Fuse	20	458
Power module	28	458
BEC	10	537
HearLink airUnit	70	537

Table 6 continued from previous page

Component	weight (gram)	distance from nose (mm)
Wing	800	642
Telemetry	12	655
BEC	10	655
Pixhawk Cube	35	655
telemetry	12	744
RX	6	744
GPS	40	822
Landing Gear	100	822
Raspberry pi	46	973
BEC	10	973
ESC	100	1181
Tail	200	1328
Rudder	120	1300
Motor	400	1480
fuselage	900	1527

Table 6: Weight Distribution

CG at 150mm from the wingtip.

4 AUTONOMOUS MISSIONS

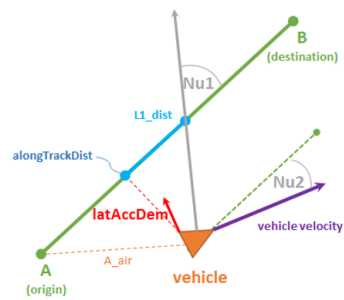
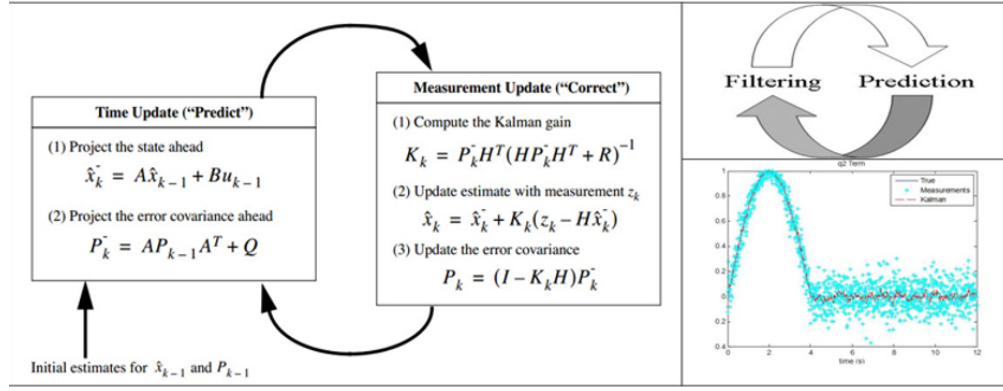
Autonomous Take-Off is planned in auto mission from mission planner, vehicle armed to trigger and start take-off mission.

Loiter Mode:

After finishing successful take-off the vehicle is going to start loitering at specific altitude with specific radius waiting for another vehicle to be launched. Vehicle won't go out of this mode unless other vehicle positions are received and proved their air-seed they are on air.

search-track mode:

Decision making of which enemy flight is near and with less (bearing-heading) angle to follow it by estimating its position and direction of motion. Ground station should decide which vehicle to follow, then send its location in real-time to an on-board system that will start to track it. On-board computer will initialize the kalman filter to predict the position of the vehicle in real-time.



alongTrackDist: distance from A to closest point on line from A to B
L1_dist: distance from alongTractDist to target point on path
 $L1_dist = 0.3 * damping * period * speed$
Nu1: angle from vehicle to L1_dist point (relative to line from A to B)
Nu2: vehicle velocity angle relative (relative to line from A to B)
latAccDem: desired acceleration output along red cross track line
 $LatAccDem = \frac{4 * damping^2 * speed^2 * \sin(Nu1 + Nu2)}{L1_dist}$

In a loop of prediction with high rate and correcting with incoming data which has lower rate; the vehicle is going to track the predicted position of the other vehicle and track it by L1 tracker.

4.1 Autonomous Lockdown

During the search-track mode we are trying to detect the other vehicle using the image processing YOLOR algorithm and starting fight mode when first confirmation of existence is done. In fight mode, we continue using YOLOR

that works to bring and keep the target into the field of view by following the target. Confirmation of target existence is done by detecting it using image processing YoloR algorithm then start locking.

YOLOR algorithm:

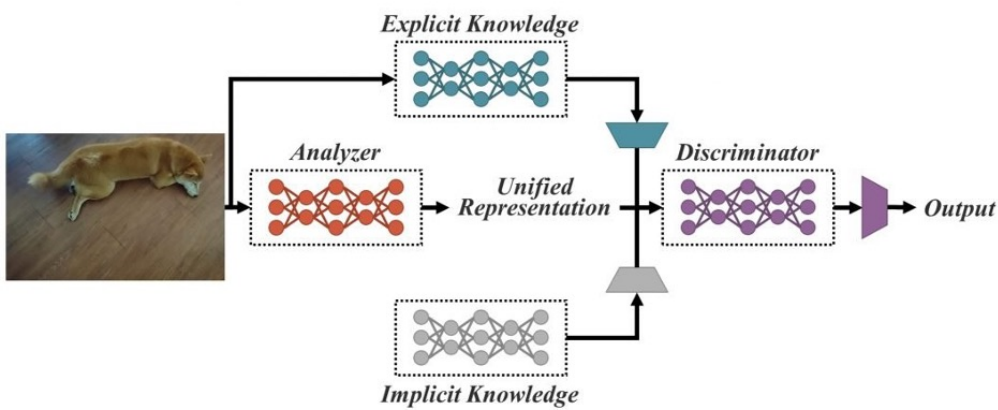
Because of the differences in authorship, architecture, and model infrastructure, YOLOR is a state-of-the-art machine learning algorithm for object detection. It differs from YOLOv1-YOLOv5. YOLOR stands for "You Only Learn One Representation," not "You Only Look Once," as in YOLO versions 1-4.

Object detection is the sole purpose of YOLOR, as opposed to other machine learning applications such as object identification or analysis. This is because object detection is based on general identifiers that classify an object into a certain group or class.

Humans may learn and understand the physical world by vision, hearing, and touch (explicit knowledge), as well as previous experience (implicit knowledge). As a result, hu-

mans can efficiently interpret wholly new facts by drawing on a wealth of prior learning experience that is earned through normal learning and stored in the brain.

The YOLOR research article is founded on this concept, and it offers a method for combining explicit knowledge, which is defined as learning based on supplied facts and input, with implicit knowledge, which is learnt subconsciously. As a result, the YOLOR concept is based on simultaneously recording implicit and explicit knowledge, similar to how mammalian brains process implicit and explicit knowledge. The suggested unified network in YOLOR provides a unified representation that may serve a range of jobs at the same time.



Kernel space alignment, prediction refinement, and a convolutional neural network (CNN) with multi-task learning are three notable procedures that make this design functional. According to the findings, adding implicit knowledge to a neural network that has already been trained with explicit knowledge improves the network's performance on a variety of tasks.

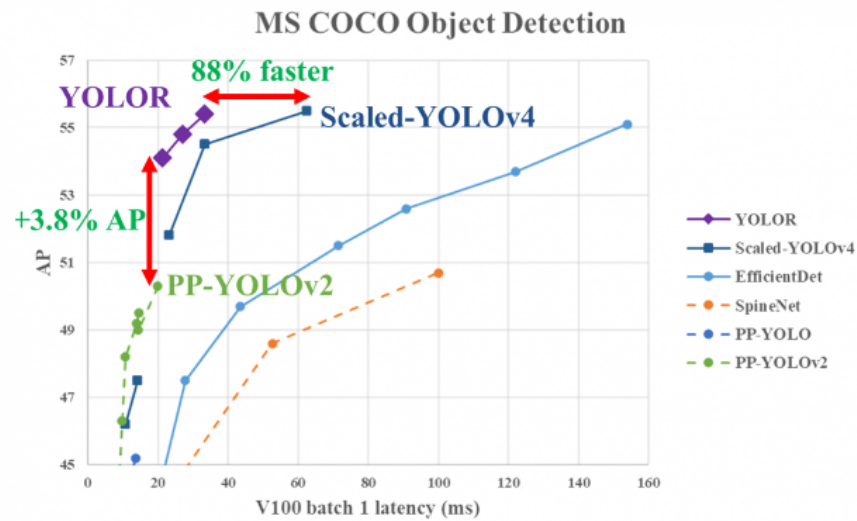
Multitask learning contains tasks such as object detection, multi-label picture classification, and feature embedding. That is why we selected YOLOR

Convolutional Neural Networks (CNN) are typically used to achieve a single goal, but they may be trained to tackle numerous issues at once, which is exactly what YOLOR is aiming for. CNNs are frequently built with a specific purpose in mind. YOLOR aims to have CNNs learn both (1) how to get outputs and (2) what all the potential outputs could be, while CNNs learn how to evaluate inputs to produce outputs. It can have multiple outputs rather than simply one.

YOLOR accuracy and performance:

The novel YOLOR algorithm seeks to complete jobs with a fraction of the extra expenses that comparative algorithms are expected to incur. As a result, YOLOR is a unified network capable of processing implicit and explicit knowledge simultaneously and producing a refined general representation as a result of the technique.

The YOLOR obtained equivalent object detection accuracy as the Scaled YOLOv4 when combined with state-of-the-art approaches, but inference speed was raised by 88 percent. YOLOR is one of the quickest object detection algorithms in modern computer vision as a result of this. On the MS COCO dataset, YOLOR has a 3.8 percent greater mean average precision than PP-YOLOv2 at the same inference speed.

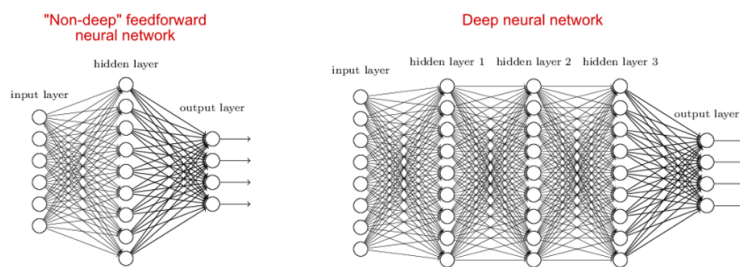


YOLOR explicit knowledge:

These are fact-based data that could be obtained with the use of shallow neural networks. Explicit knowledge is the result of conscious learning.

YOLOR Implicit knowledge:

Implicit knowledge is the extraction of detailed features from provided data, whereas explicit knowledge is the extraction of rough features. Deep neural networks can be used to extract implicit knowledge. Implicit learning is the result of subconscious learning.

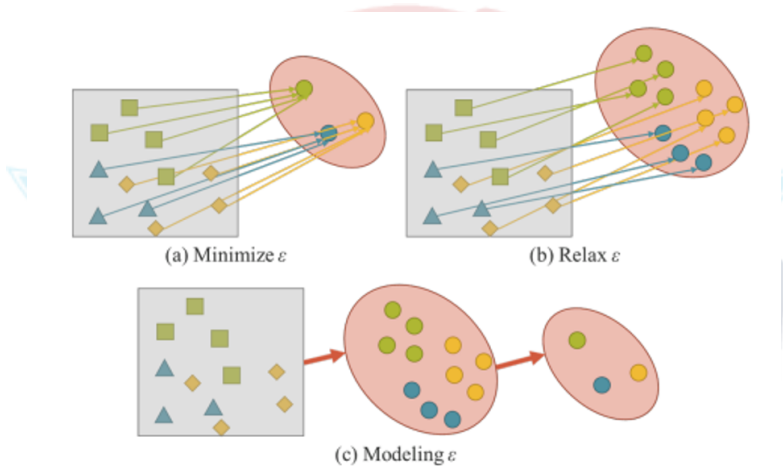


When implicit knowledge is combined with explicit knowledge, performance in tasks such as kernel space alignment, prediction refinement, and multitask learning improves.

In general, a neural network serves only one purpose, hence different neural networks are required to do diverse tasks. By combining implicit and explicit knowledge, YOLOR solves this limitation and serves the aim of multitasking and achieving numerous objectives at the same time.

$$y = f_{\theta}(\mathbf{x}) + \epsilon \longrightarrow \text{minimize } \epsilon$$

In the previous formula, y represents the task's target, x represents the observation, (θ) represents a collection of neural network parameters, and f represents the function that performs the provided operation. The error rate, on the other hand, is represented as (Epsilon). The error rate must be reduced constantly. To meet the provided goal, the error rate (ϵ) must be kept to a minimum. The relaxing of ϵ is done to achieve the generalization of the model being able to solve all problems in domain T, and finally the modeling of error rate is done to obtain t_i .



Implicit and explicit knowledge general formula:

$$y = f_{\theta}(\mathbf{x}) \star g_{\phi}(\mathbf{z}) \quad (7)$$

Using the combining operator, the implicit and explicit knowledge formulations are combined. The addition or concatenation operator is used as a combining operator.

Modeling Implicit knowledge:

Implicit knowledge can be represented in three different ways:

1. Vector: used as an implicit representation
2. Neural network: uses vector and adds weight to it then uses linear combination or non linearization for representing implicit knowledge.
3. Matrix factorization: Multiple vectors are combined as an implicit representation of knowledge using a prior base of knowledge and a coefficient.

Vector is used as direct implicit representation and Detection results are as in the following figure, and errors from the center of the frame are calculated.

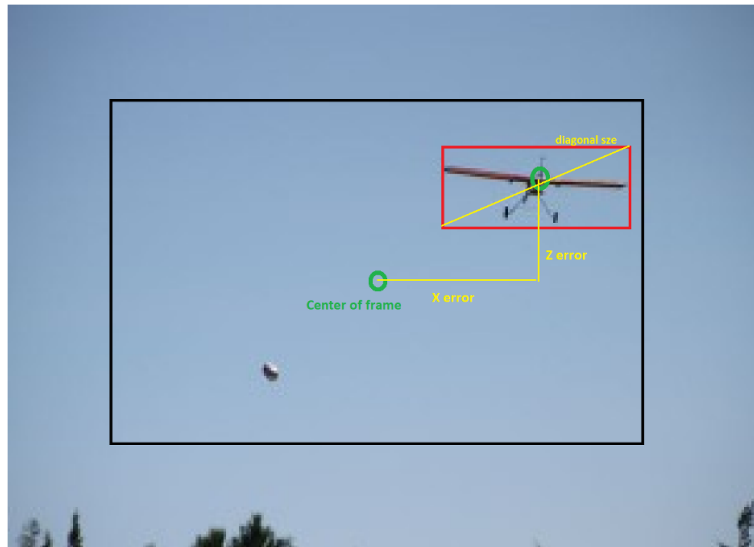


Figure 12: Image error calculation method

After first detection, fight mode started and a kalman filter with two measurements (Enemy's location based on frame pixel position estimator, and detection result) initialized to predict then track the position of the enemy in the frame (in pixels) with high rate and smoothed output. Error of prediction output is calculated as the above image too. High rate control loop of 20 HZ should take place.

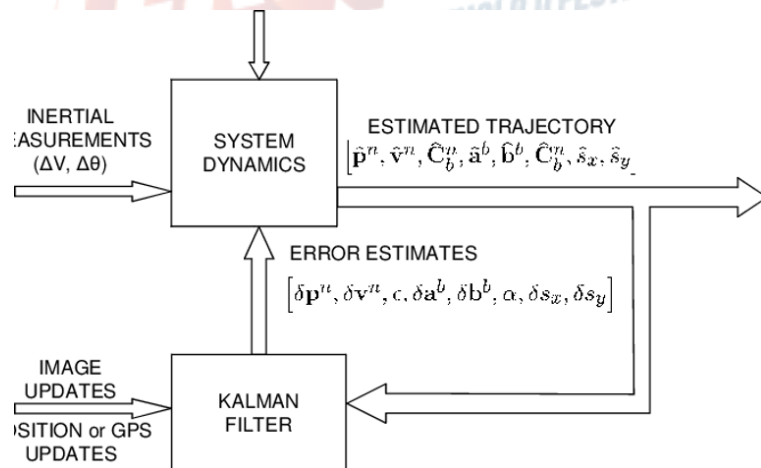


Figure 13: kalman filter algorithm

After error calculated, vehicle attitude control diagram is as following:

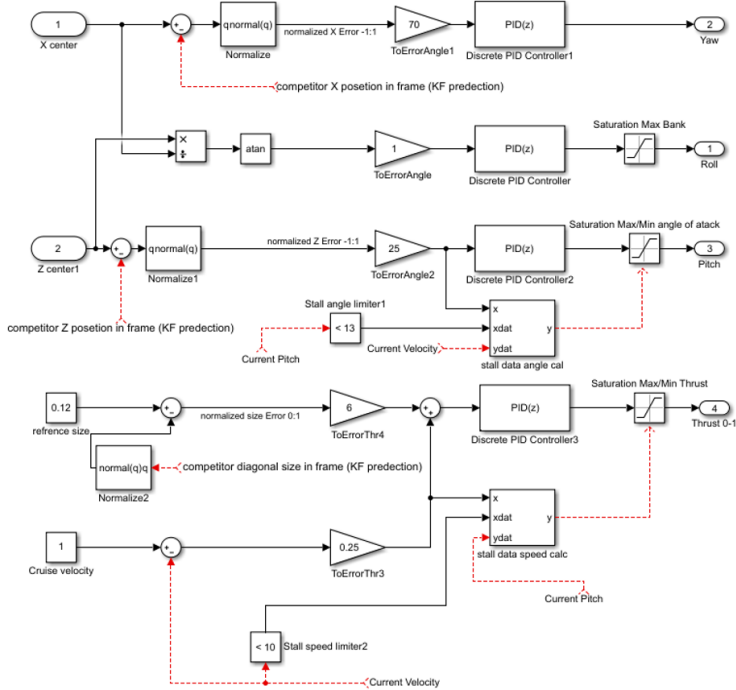


Figure 14: vehicle attitude control diagram in dog fight mode

All errors are normalized with the frame size and multiplied by maximum acting angle. In the simulation environment PID coefficient tuned for smooth rapid attitude tracking. multiplied angle is changed with the change of the linear displacement of the enemy's vehicle from ours to have these shown maximum angle at the most near displacement of 10 m. and divided by the (displacement/10).

prevent from stall functions with stall speed angles data is used in throttle control and pitch control to prevent stall either from high angle of attack or stall speed.

4.2 Kamikaze Mission

$$\text{descentangle} = \text{atan2}(\text{attitudedifference}, (\text{XY})\text{diagonaldifference}) \quad (8)$$

Where,

θ = bearing angle between UAV location and QR location - UAV's heading angle

With these calculated angles errors PID attitude controller loop takes action to compensate for these errors. Beside these errors, the thrust control will try to keep up a reference velocity.

In the simulation environment PID coefficient tuned for smooth rapid attitude tracking. Filter for attitude prediction may be used for a high rate control loop of 20 HZ.

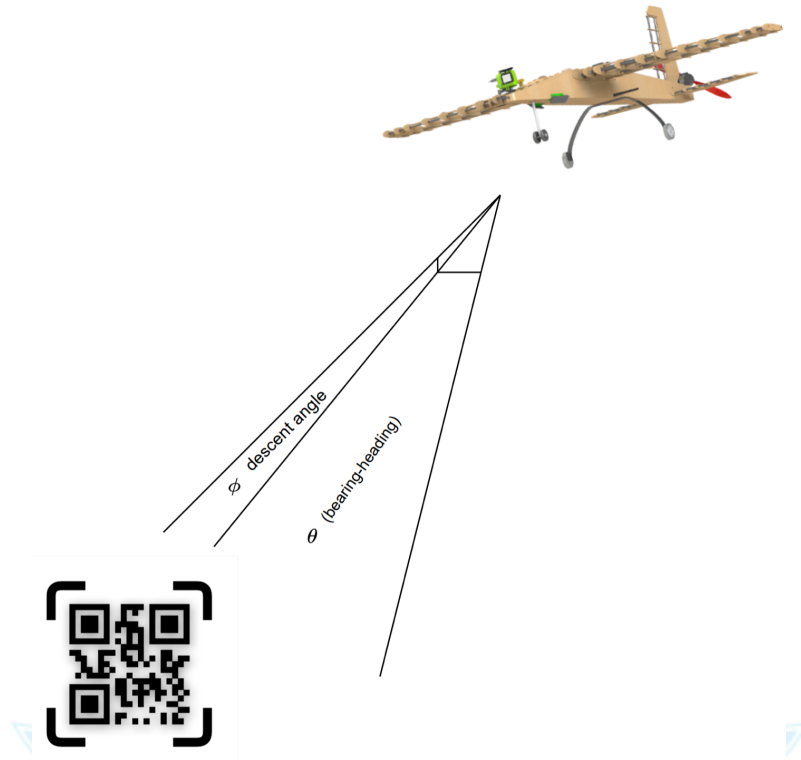


Figure 15: descent attitude error calculation

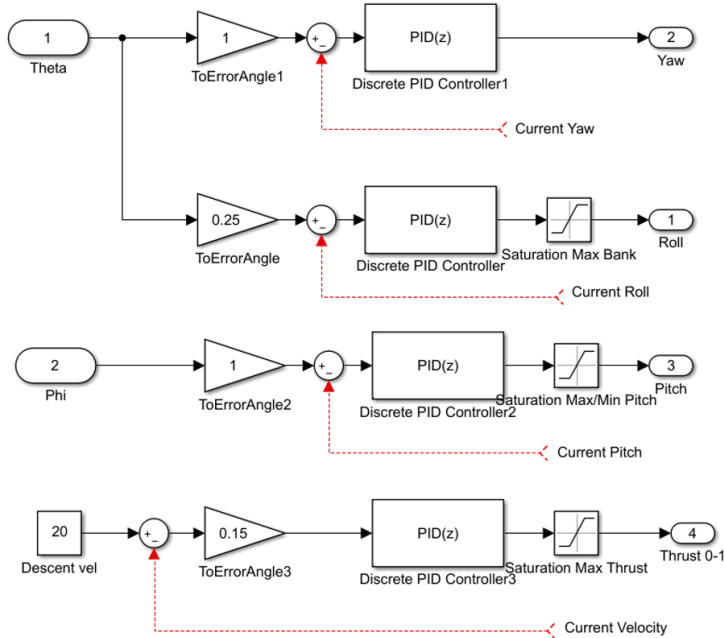
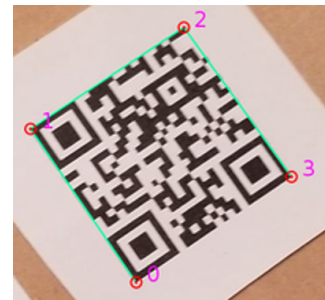
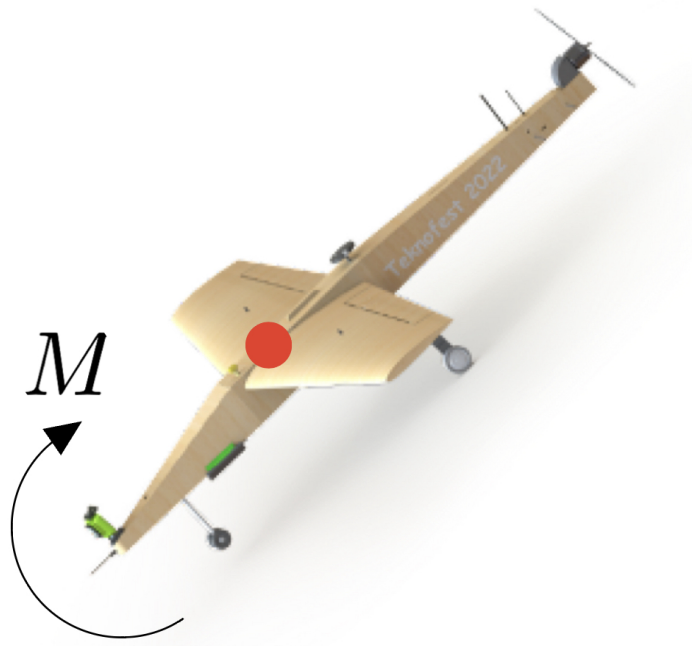
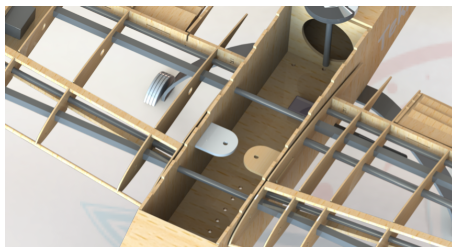


Figure 16: vehicle attitude control diagram in dog fight mode

With the Zbar QR read, detect and encode library with OpenCV, QR code pose in frame will be detected and read then encoded and sent to the competition server. when QR detected encoded data with lock information sent to the server.



To achieve the mission we need to dive at speed 8 m/s and 25 degree angle. Then we need to recover before touching the ground. While recovering the CG region will reach a high stress level. So the wing and the fuselage are susceptible to being broken. As a result, this critical region is reinforced in the fuselage and the wing is by carbon fiber cloth which has a yield strength equal to 2500 MPa.



5 GROUND STATION AND COMMUNICATION

RabbitMQ:

RabbitMQ is a message broker that will be used to establish a communication between different interfaces and modules of the aircraft which should result in a much cleaner structure compared to making the modules communicate directly to one another. The desired result is isolating each module of the aircraft and routing all the communications through the RabbitMQ.

General structure:

Modules are divided into two main groups (Ground station and plane). On the Ground Station there are the image detection module, message broker, maps module, flight control module, finally the database module.

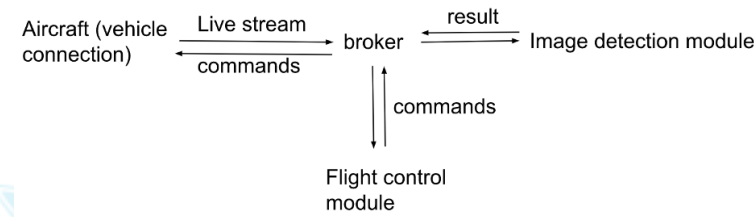
While on the plane there is just the live video module which is connected directly to the on board cameras also there is the vehicle connection module which handles communication between plane and ground station.

- Communication with the jury's server:
 - The jury's server publishes data to the RabbitMQ module on the other side both the ground station and the maps modules are subscribed to the jury's data through the broker module. This results in the locations of the rival aircrafts displayed using the maps module while the necessary calculations are being computed on the ground station module. The broker can also publish to the jury's server the current location of the aircraft and the live stream. So both the jury's server and the ground station are publishers and subscribers to each other through the message broker.
- Communication between aircraft and ground station:
 - On the plane there is a vehicle connection module that sends and receives the data between the plane and the rabbitMQ broker on the ground station. The broker is required to handle which module on the ground station receives the coming data. For example as mentioned above when the aircraft sends its location the broker should direct it to a couple of channels one of which is the jury's server.
- Communication between different modules on the ground station.
 - On the ground station channels are created by the message broker and modules would be either subscriber or publisher or both to these channels.

Examples would be:

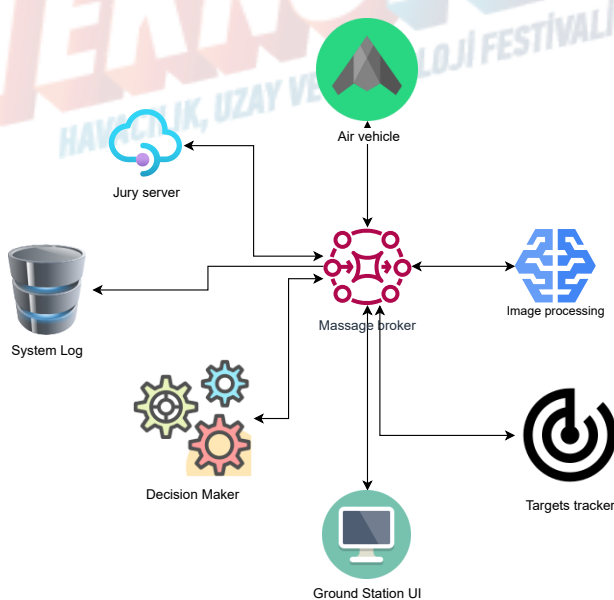
Between the image detection module and the vehicle connection module, initially the vehicle connection module will send the live video to the message broker on the ground station which will direct it to the image detection module. After the rival aircraft is detected the result should be passed back to the broker which will be directed to the flight controller module which will make a decision and send the command back to the broker which will finally pass it back to the vehicle connection module in order for the aircraft to execute the command.

Another example is the connection between all the modules and the database module. All modules would send all the messages - such errors, faults and successes - to the broker which will pass it to the database module to log it.



The protocol which all the above communication would go through is MQTT.

MQTT is a light weight broker protocol that follows the publish/subscribe model to provide a message protocol for minimal network bandwidth application ex. (iot applications).



Communication diagram between ground station and on-board system is relayed on multi-spectrum redundant and independent chart;

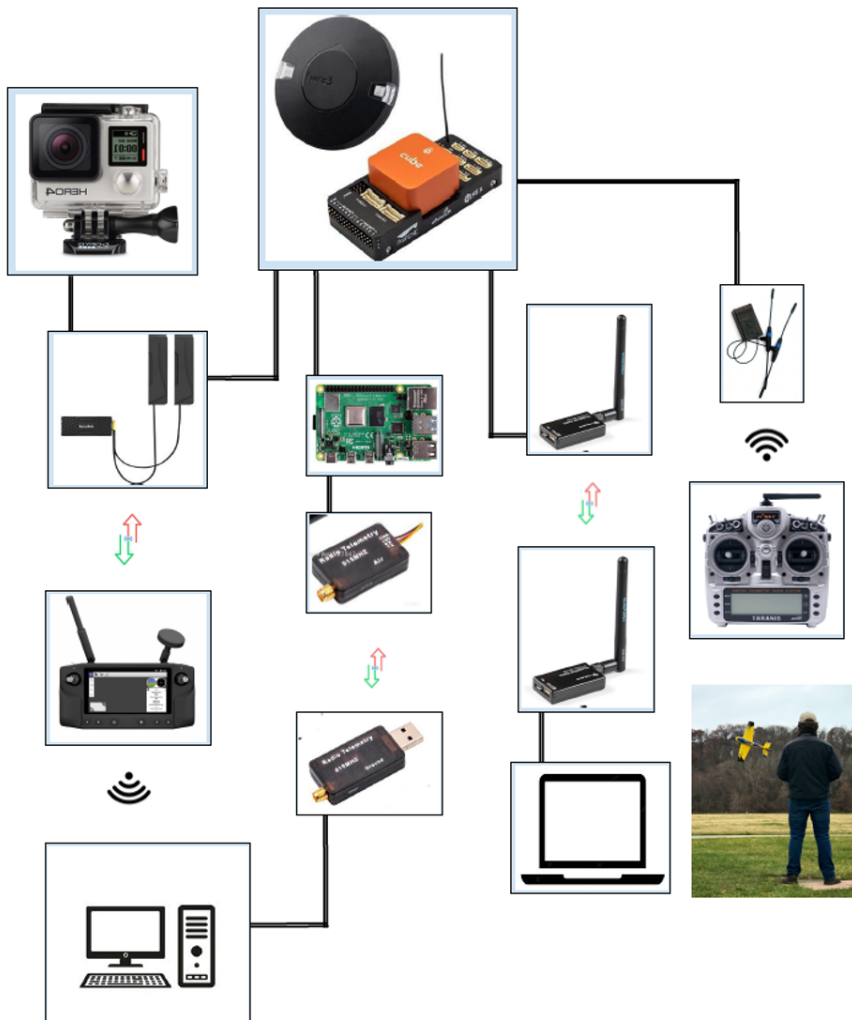


Figure 17: Communication Diagram

- Remote controller: We decided to use the Frsky x8r RC receiver to connect the UAV with the pilot to have manual control of the UAV. It has 16 channels with 8 channel PWM and all 16 channel dedicated S.BUS.
- HereLink is a device we chose to provide telemetry data to ground stations and to ensure access to the camera of UAV. in real time at a high rate. It has 2 HDMI ports for cameras with 1080p for 30fps/60fps .It transmits data over 20KM with minimum latency 110ms. It has a processor with eight core performance named S1. In addition Solex and QGS which are two types of GCS we can choose among them. So HERELINKE could be concluded as professional UAV monitoring and datastream link.
- Telemetry data which connects UAV to pc. It has around 3 km range, 433mhz and 1000mw. With the telemetry module we will configure the drone in the mission

planner and assign the parameter. Also will be used to monitor the vehicle on air and command it in case of system failure.

- RF 915 Mhz channel to send mode data, enemies location data, detection results, and main control commands to the companion computer is used to ensure real-time reliable in motion data feed to on-board system.
- GPS receiver: Here+ is used for 50cm accuracy of position with high frequency of 5-10 Hz.

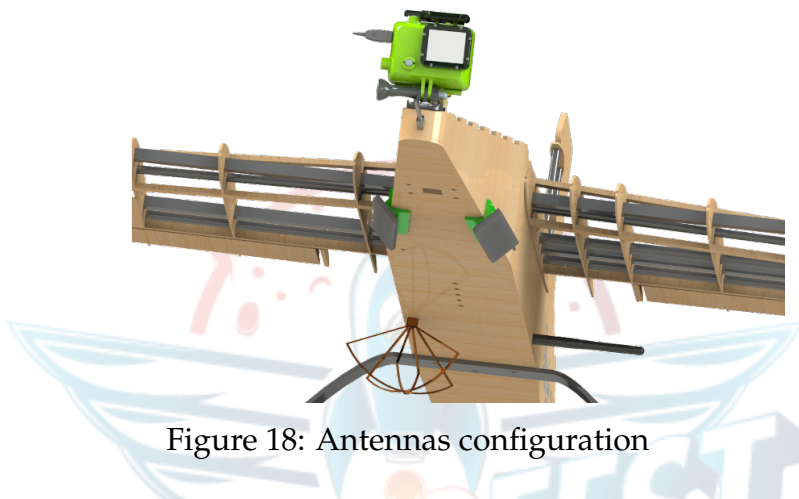


Figure 18: Antennas configuration

All antennas are configured and placed on the bottom and oriented to ensure coverage in all cases, also the receiver antenna is placed to be free held from bottom to freely move and ensure good orientation facing the remote control transmitter antenna.

Frsky R9 receiver is 16 channel with high gain receiving antenna ensuring coverage all time and in all orientations.

Circular polarized antenna:

No matter what direction or angle your mini quad is flying at in relation to your receiving antenna, circular polarized signals always overlap (no signal loss regardless of the antennas alignment is). Circular polarized antennas have therefore become the industry standard in FPV flying. It also has the benefit of being able to reject multipath interference. The most prevalent cause of poor video quality is multipath interference, which manifests itself as unpredictable color changes, static, confused images, and drop-outs. When a signal is reflected from an object, it becomes distorted and phase delayed, interfering with the main signal. Left-hand circular polarized antennas (LHCP) and right-hand circular polarized antennas (RHCP) are two types of circular polarized antennas (RHCP). The antennas on the transmitter and receiver must be compatible; otherwise, severe signal loss may occur. It's good for Low altitude flying -Acrobatic flying when the aircraft's attitude and angle are continually changing (proximity flying)

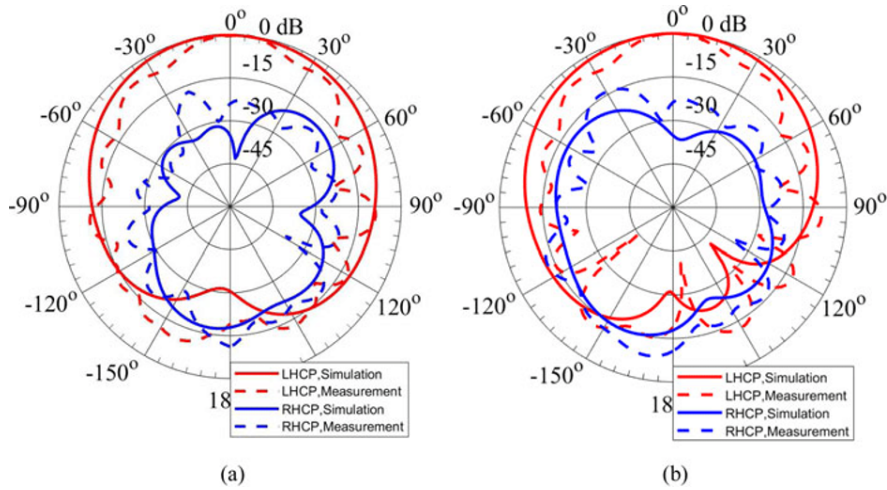


Figure 19: circular polarized antenna gain with angles in two planes

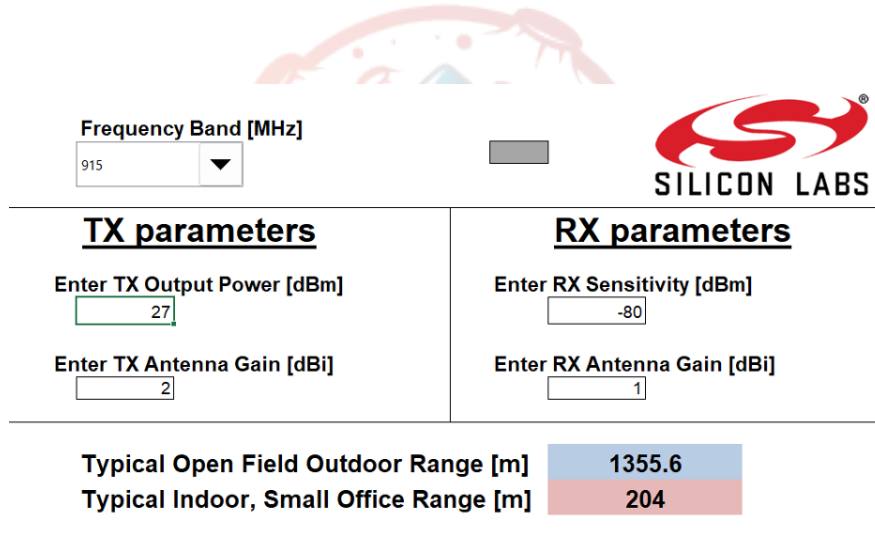


Figure 20: range calculator of the device with worst cases and sensitivity

Herelink antenna:

- Frequency Range: 700-800MHz / 824-960MHz / 1575.42MHz / 1710-2170MHz / 2400-2800MHz
 - Input Impedance: $50\ \Omega$
 - VSWR: $\leq 2.5:1$
 - Radiation: Omnidirectional
 - Maximum Power: 50Watts

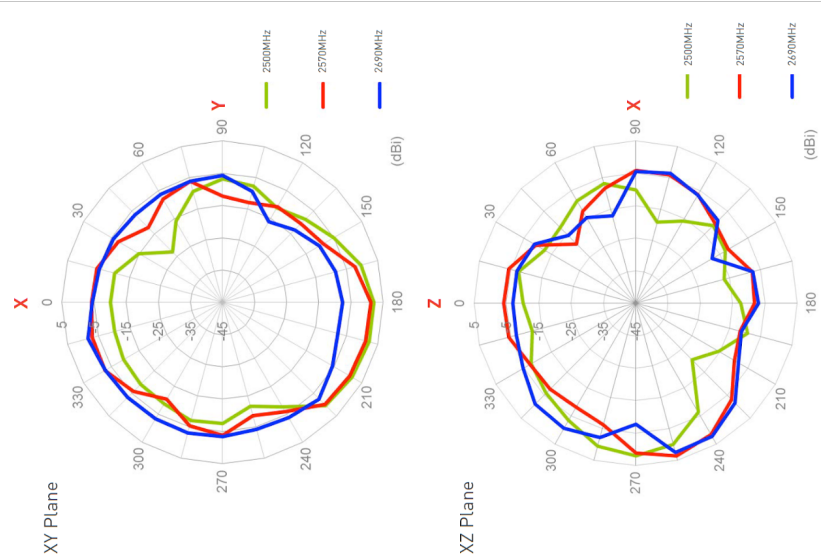


Figure 21: antenna gain with angles in two planes

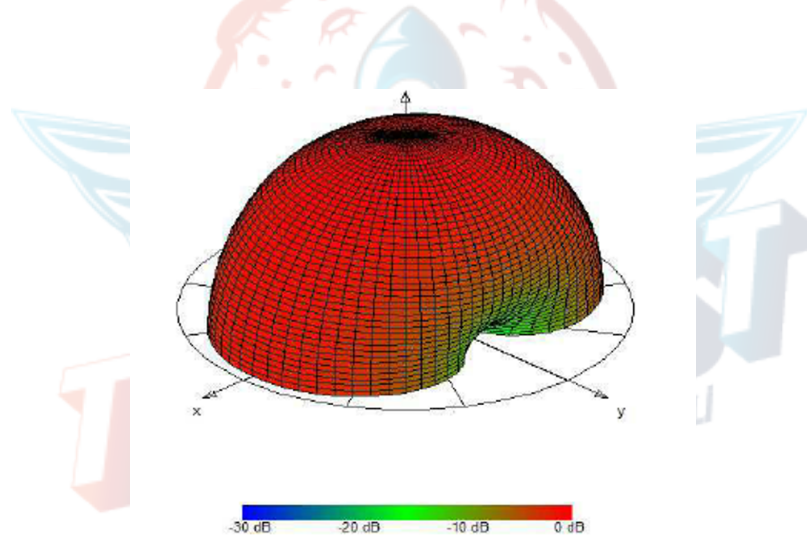


Figure 22: antenna gain with angles 3D

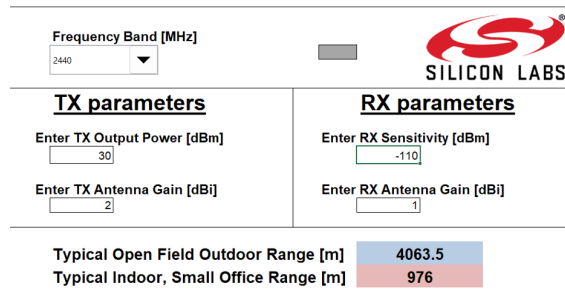


Figure 23: range calculator of the device with worst cases and sensitivity

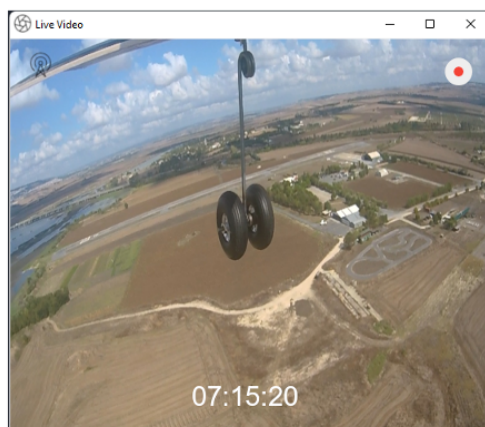
6 USER INTERFACE DESIGN

Like shown in the communication-interface diagram in figure 17 there is three interfacing units on the ground with on-board system/UAV;

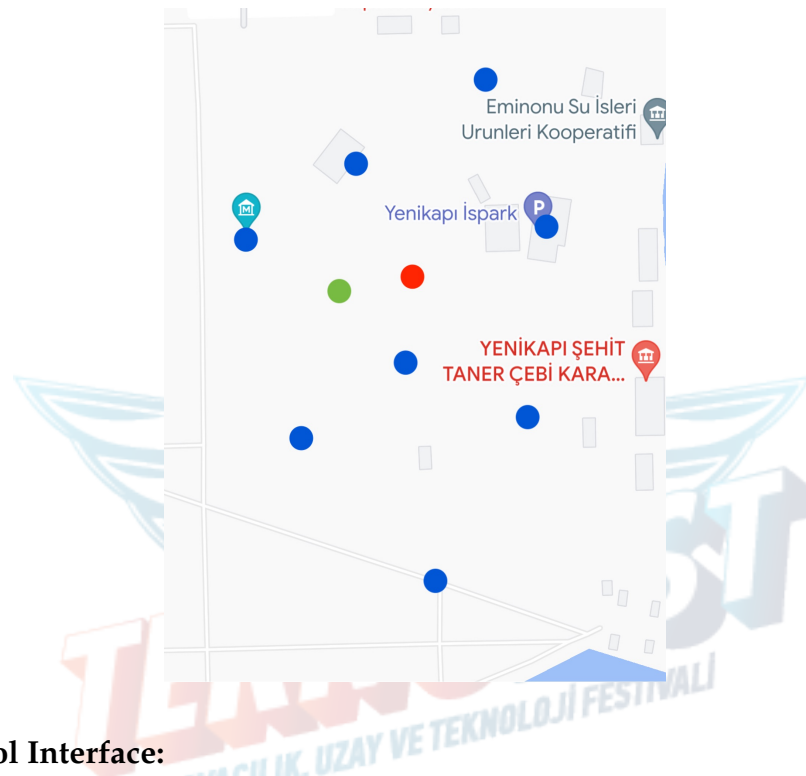
PC interfacing:

- Camera Interface:
 - The camera interface is considered to be one of the simplest interfaces as it only contains the live video from the aircraft. Its two main responsibilities are to monitor the live video or to display the detection and lock of the target aircraft while in the fight mode. In addition to that the interface will show the time of the flight and the state of both recording and broadcasting.
- Monitoring:
 - For monitoring the live video should be constantly showing on the screen in real time as it could be used to manually control the aircraft if needed at any given moment. The live stream also should be broadcasted and sent to the jury server, such action will be achieved by sending the stream to the message broker (RabbitMQ) which will handle sending it to the jury's server separately.
- Detection and locking:
 - While the aircraft is in searching or fighting modes the live video should show the rival aircraft surrounded by a rectangle which should be drawn as soon as a rival aircraft is detected in our FOV and it should be drawn by the ground station. While the aircraft is trying to maintain a successful lock on the rival aircraft a recording of this process should be initiated and saved on the ground station to be sent to the jury's server. The camera interface should alert the user that a recording is taking place at the moment.

Example of the interface:



- Map tracker UI:
 - This is a real time map that gives information about enemy aircrafts relative to our aircraft position, every aircraft is represented by a spot on the map, our aircraft is represented by green color, target aircraft is represented by red color and other aircrafts are represented in blue. This gives us the ability to understand in real time how our system works and if it's functioning in the right way.



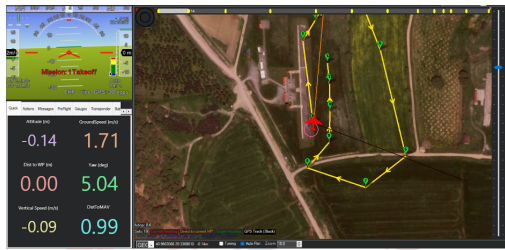
Remote Control Interface:

- 4-axis Joysticks to control thrust, yaw, roll, pitch in manual control modes.
- Two three position switches to change between different flight modes and to switch to manual, return to launch, or failsafe fall in case of emergency.
- Analog channels used to tune the control coefficients on air.

Mission Planner laptop: The following image shows the mission planning interface of the mission planner where takeoff points, pitch angle, loiter and autonomous navigation waypoints, and landing approaching points with altitudes and land points are located. Also, the radius of the waypoint that it's considered reached is specified. Different maps and hybrid maps could be selected. Also, the polygon fence, which is the border of the flight area, is drawn and uploaded from this page.



The main page where real time attitude, velocity position of the vehicle could be monitored.



Actions menu where basic actions of arm/disarm, level sensors attitude estimator initialization, and mode change is made.



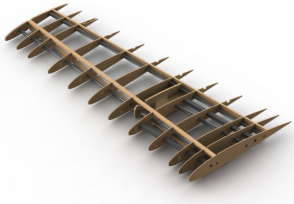
The basic tuning of coefficient, attitude limitations, and cruise is defined.



7 AIRCRAFT INTEGRATION

7.1 Structural Integration

Wing:



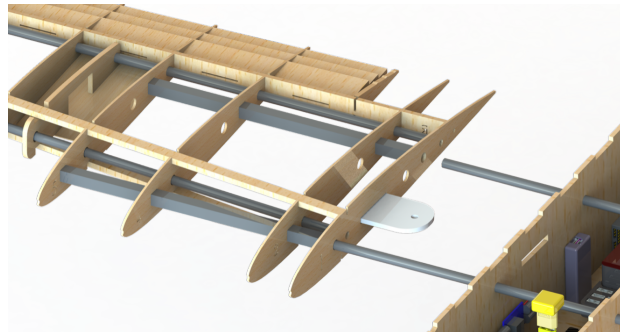
The wings of our UAV are made out of balsa and carbon fiber. Using a CAD design program to model a 3D wing and export 2D files ready for laser cutting. Then, assemble the balsa ribs with the carbon fiber rods, using fast adhesive and epoxy to fix them together. Using balsa sheets to

cover the surface of the wing and sanding the sheets very well to be ready for shrinkable skin covering .Furthermore, covering the wing with heat shrinkable skin provides high strength, a smooth surface, and good shape.



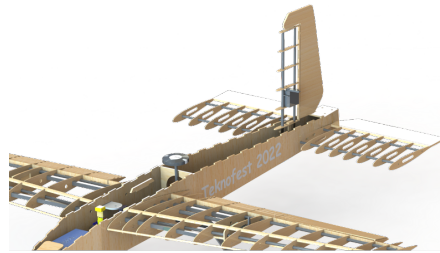
Based on the simulation that we have made (shown in simulation and test section), the AFT-SWEPT wingtip is chosen. So, The PLA 3D printed AFT-SWEPT wingtip is glued with the wing using epoxy and covered by heat shrinkable skin.

Carbon fiber rods are used to integrate the wings to the fuselage. So, it's easy and fast to be assembled and disassembled. And this white 3D printed part is used to prevent the wings from moving out during the flight. So, it can't move up and down or forward and backward because of carbon fiber rods and it can't go out because of the 3D printed part.



Tail and Rudder:

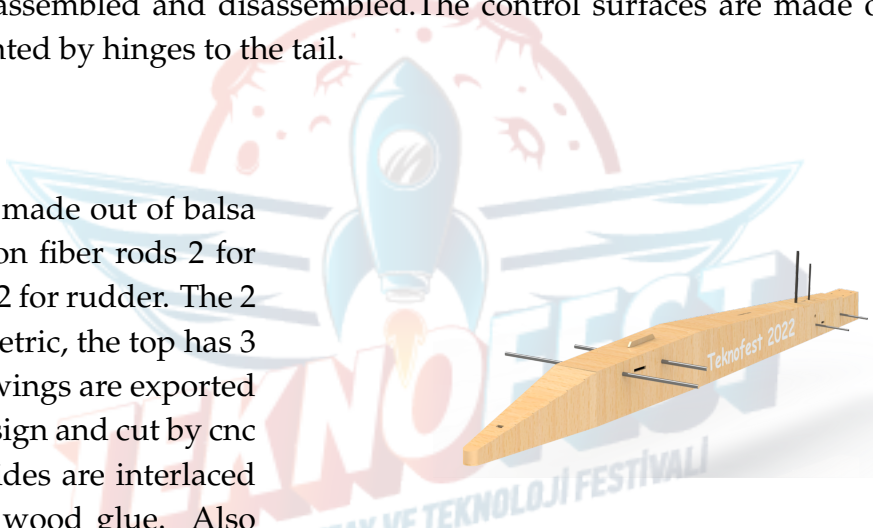
Tail and Rudder are made out of balsa and carbon fiber. And we have followed the same procedure that we used for making wings. Creating 3D design and cutting the tail and rudder into sections. Exporting 2D drawings for laser cutting. Then assembling



the balsa sections with the carbon fiber rods using fast adhesive and epoxy to fix them together. Then covering it with balsa sheets and sanding to be smooth and ready for heat shrink skin. Also we used carbon fiber rods to integrate it into the fuselage. So, it's easy and fast to be assembled and disassembled. The control surfaces are made out of 5mm balsa and mounted by hinges to the tail.

Fuselage :

The fuselage is made out of balsa and has 6 carbon fiber rods 2 for wings 2 for tail 2 for rudder. The 2 sides are symmetric, the top has 3 covers. 2D drawings are exported from the 3D design and cut by cnc laser. All the sides are interlaced together using wood glue. Also the critical places such as under the motor base and the main landing gear are covered by carbon fiber. Then, the whole body is covered by heat shrinkable film.



Landing gears:

The main landing gear is commercially available and it is made out of carbon fiber and fixed with the body by 2 M4 bolts. And the steering is made out of aluminum and has a shock absorber and retracting motor, so after take off it will go inside the fuselage to reduce the drag.



7.2 Mechanical Integration

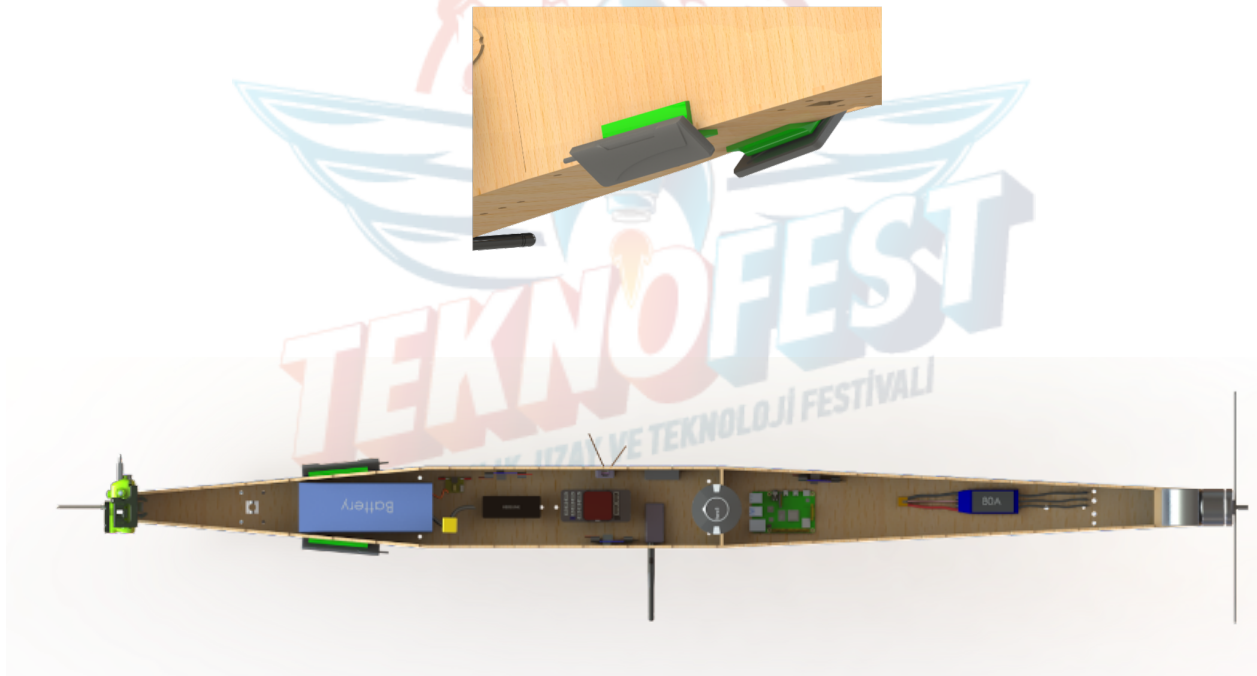
Motor:

The motor is firmly mounted on 3D printed support fixed in the fuselage rear end while taking in consideration the moment arm that could be exerted by the motor thrust.



Antenna:

The antenna of the herelink is fixed on 3D printed support at 45 degree by double face tape.



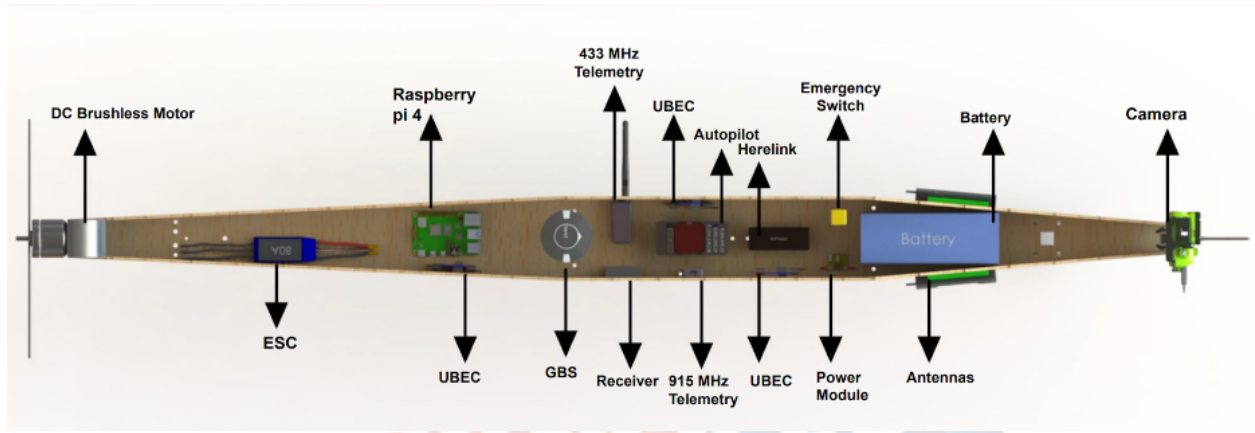
The ESC, BECs, RX, the telemetry, and the herelink air unit are fixed in the fuselage using double-faced tape. The GPS is fixed on a 5mm carbon rod, and the rod is fixed by 2 screws to the fuselage. Also, the pixhawk cube is fixed on a double plate shock absorber for the pixhawk.

The Raspberry Pi is fixed by a screw. The battery and the camera are fixed by both zip ties and velcro tape.

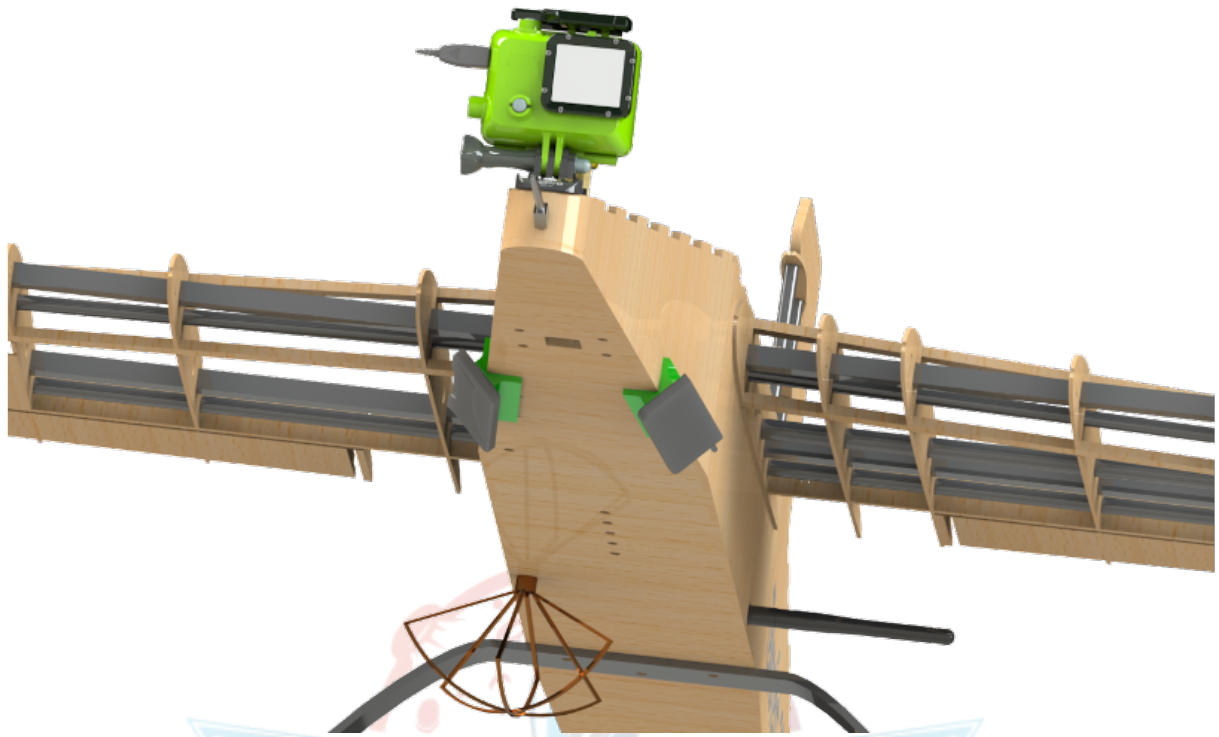
7.3 Electronic Integration

In terms of the dependability and operability of these systems, regular placement of electronic equipment in aircraft is critical. The weight of the devices, their connections, and their operation needs were all taken into account while creating the arrangement. The proper positioning of power and signal connections, in addition to the equipment employed, is critical for data security and flight safety. The electronic components of the aircraft are introduced in this part, as well as their location in the aircraft and their connections.

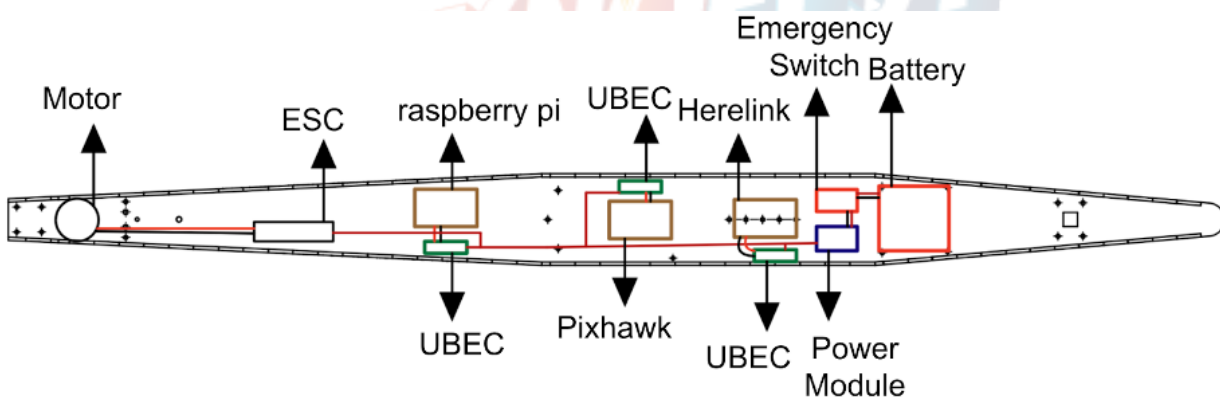
The pre-stated final system architecture components discussed in section 3.1, have been installed into the fuselage considering the proper positioning of power and signal connections.



The camera is installed into the nose of the UAV due to the competition specification. The battery is installed into the nose to tune the center of gravity point. Emergency switch has been installed between the battery and the power module. Herelink, Pixhawk, GBS, and the Raspberry pi have been distributed along the fuselage. Each UBEC has been installed beside the component it supplies and the ESC has been installed in the tail to power up the DC brushless motor. The volume of the UAV's fuselage is well balanced to contain all the components and power/signal connections.



The herelink antennas are installed in the bottom nose of the UAV to cover all the angles during the maneuvers, and the circular antenna has been installed in the bottom center for the same reason.



For power distribution, the Pixhawk 90A power module is used. The emergency switch is capable of cutting the power in less than 0.7 ms in case of an emergency and is installed outside the fuselage. It is easily reachable and yellow in color. The wiring has been organized inside the fuselage and 20 awg cables have been used for the servo motors, 18 awg cables have been used for the UBECs, 14 awg cables have been used for the motor ESC, and a 10 awg cable is used for the main power line to withstand the current. All the wires are silicon for flexibility.

8 TEST AND SIMULATION

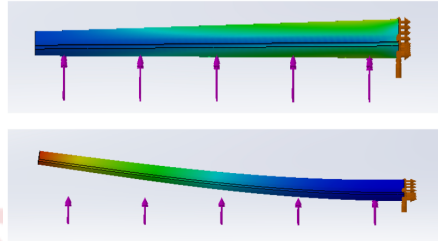
8.1 Sub-System Tests

Wing load test:

Structural Test:

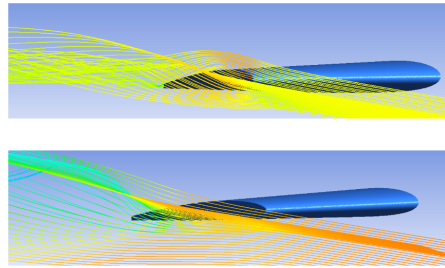
The purpose of this test is to simulate the aerodynamic loads that occur on the wings during flight and to prevent any failure that may occur. So, we have made a structural simulation using Solidworks to check the stresses on the wing. So, by adding the weight of the UAV (42 N) to half of the wing. As a result, at the wingroot the minimum factor of safety 2.1 and the maximum deflection is 40mm at the wingtip which provides 3 degrees of a dihedral angle which increases the lateral stability and the flight performance. Also after building the UAV we have made a real wing load test to compare between the computed results and the real ones. So we have put the wing tips on two chairs and increased the weight of the UAV by 4kg so the total weight is 8 kg. As a result we have a successful wing load test mathematically and by experiment.

The following image shows a wing load test to check the structure and the strength of the wing to hold the vehicle weight in the air. a small dihedral angle like the simulated one has shown.



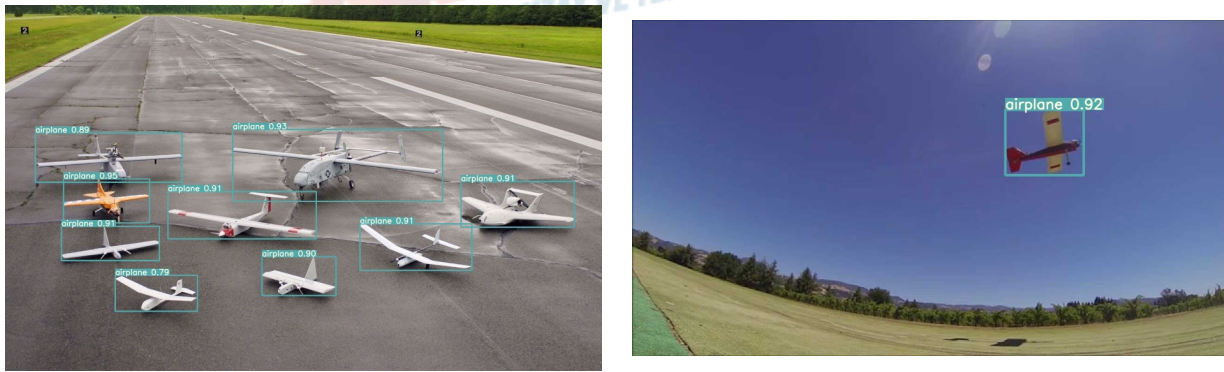
CFD simulation:

According to Bernoulli's principle: higher pressure regions have lower fluid speed and lower pressure regions have higher fluid speed. Because of the difference in pressure between the upper and lower surfaces of a wing vortices will be created which increases the induced drag. Usually winglets are used to reduce the vortices but that means extra weight will be added which is undesirable. So, using Ansys (fluent) we were able to simulate the performance of the vortices at the wingtip. The purpose of the simulation is to find proper wingtip shape to reduce the vortices as much as we can. And the difference is clearly noticeable between the CUT-OFF wingtip and the AFT-SWEPT wingtip.



UAV YOLOR detection:

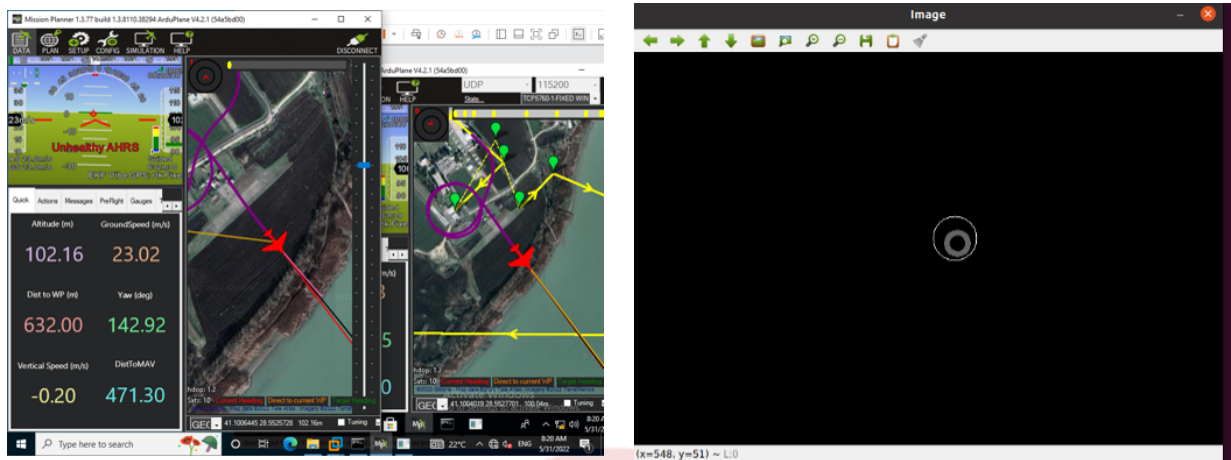
YOLOR detection tested to achieve fps of 10 at low power GPU (low power GTX 1050) at laptop achieve 12 FPS with 80 class complicated model. Despite this fact we are training our model of one class tiny mode that will achieve more than max stream fps of 30 on our ground station PC with (GTX 1070 8GB or RTX 3060 12 GB) high power graphic card. YOLOR tested in a lot of pictures to prove that it's the best choice for small size objects in the frame with high confidence and fps rate fit our need.



Dogfight tracking:

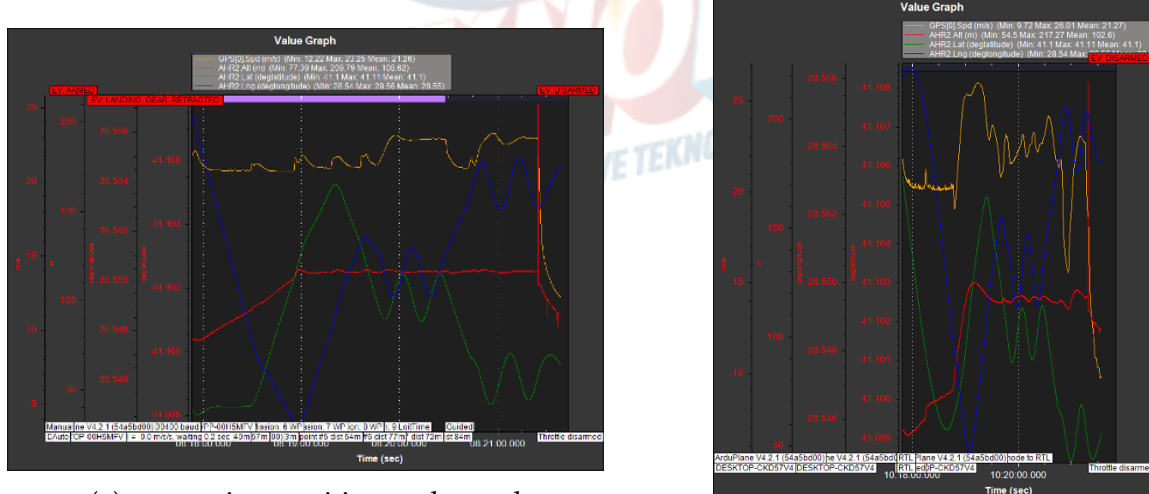
Simulation of dog-fight tracking is made by simulating two independent vehicles on SITL with visualization on mission planner and plotted graph. Used camera focal length is

multiplied by the displacement of the enemy from our vehicle in the body coordinate frame to give the enemy's place in the camera frame in pixels.



(a) screenshot of two simulation plane in dog-fight mode (b) simulated competitor detection using positions and camera focal length

When the object size in the frame is more than 2%, it is tested to be detected in detection model dog-fight mode initialized with the simulated detection and kalman filter for prediction and tracking with a high rate.



(a) competitor position and speed

(b) vehicle position and speed in tracking

The PID controller is primarily tuned to control the enemy's vehicle in high speed tracking and nearly smooth with no hard turning to avoid instability and high G-force. Tracking for 10 seconds made successfully multi-times in the simulation and the following image shows the response (attitude of the simulation of our vehicle).

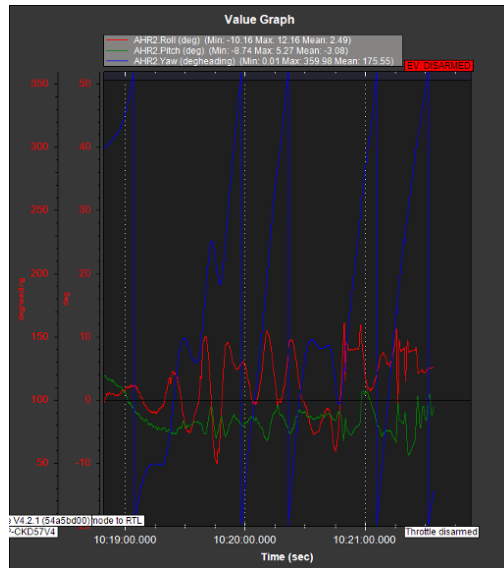


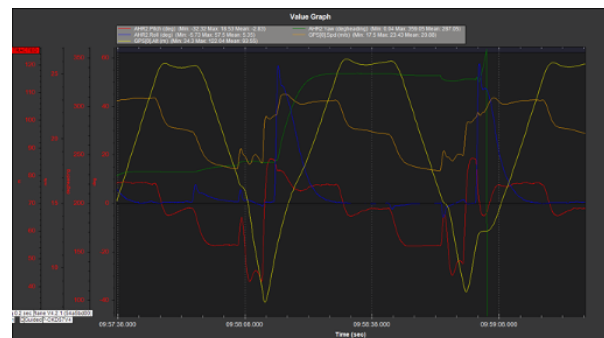
Figure 27: vehicle attitude angles in tracking

Kamikaze:

kamikaze mode simulated in SITL by predefined four points at the corner of the flight area. During loiter flight displacements and angles to each point is calculated and weighted by priority to climb and bearing angle then displacement and so on. when the total weight exceeds the threshold nearest and easiest to go point is targeted to go. In Kamikaze fight-mode ratio of climb and bearing angle to distance to the point of start fighting is calculated with formula and if it exceeds threshold the vehicle loiter to ensure good heading perpendicular heading to QR code point to be able to lock on. When some criteria are achieved the vehicle enters the attitude control mode to descend toward the QR code. It starts the descent from altitude of 100 m to ensure lock is done by altitude of 40 m. The following image is a plot of two consecutive points of lock, when lock period is done, climb control is made to ensure the vehicle gains velocity and altitude to not stall.



(a) screenshot of simulated vehicle during kamikaze mission



(b) vehicle attitude angles and altitude in two consecutive kamikaze missions

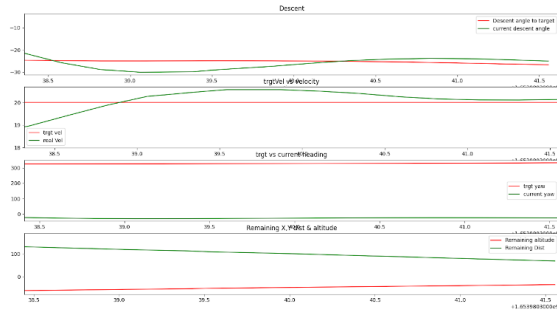


Figure 29: kamikaze descent attitude control input and output

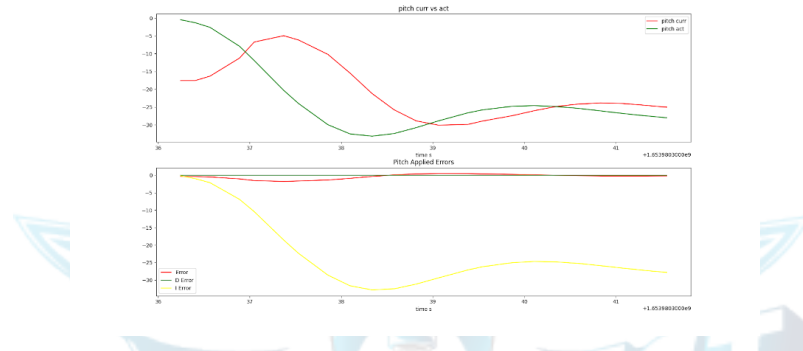
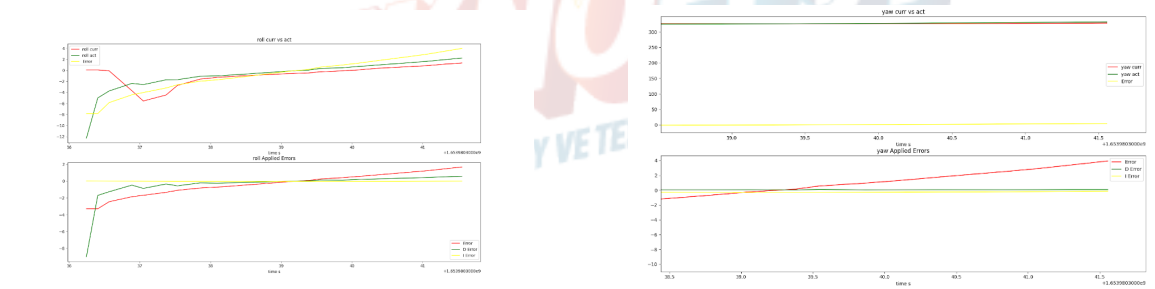


Figure 30: pitch angle control data



(a) roll angle control data

(b) yaw angle control data

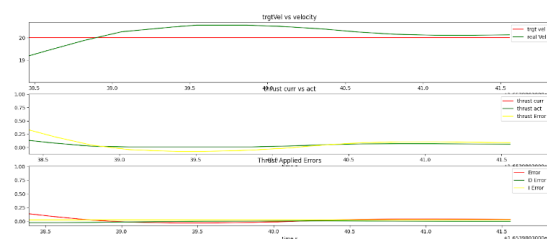
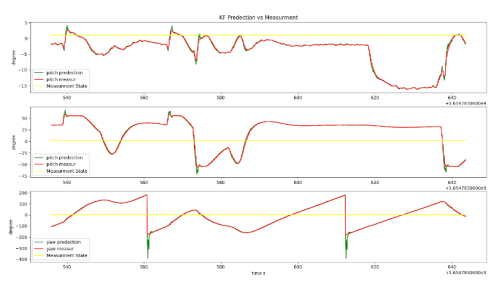
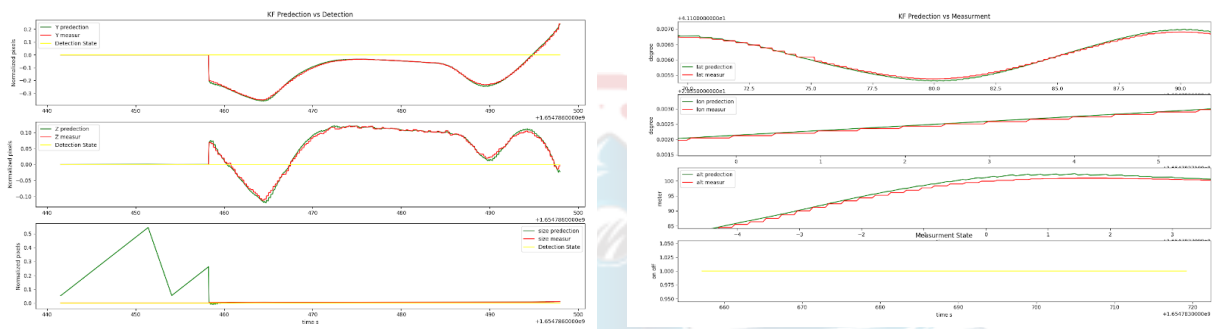


Figure 32: Velocity control dat

Attitude Kalman filter prediction is made to be able to control the vehicle at a high rate:



The Kalman filter prediction and estimation data is simulated and plotted as follows:



(a) in frame image object position prediction

(b) Global location prediction

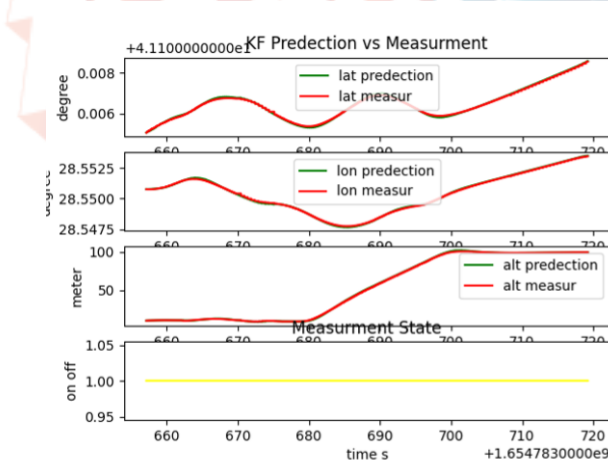


Figure 34: zoomed global location prediction shows true smooth prediction

8.2 Flight Test and Flight Checklist

Center of gravity tests performed:

multi tests performed to ensure the center of gravity is stable and not heavy nose. Because the criteria of stability needed to be not too high to give the vehicle the ability of easy maneuver and to minimize the size hence the weight of the fuselage, the first design Cg is made in the end of Cg region. After multiple tests of take-off and stall because over back placed Cg, a good point for Cg is defined and tested for stable flight. Because it would be too long a fuselage to maintain Cg at 10 cm from the tip of the wing or 55cm distance from end of wing to tip of tail, tail area is enlarged to have the Cg at 14 cm from tip of wing. Like it clarified in section 3.4. So changes were made on the fuselage and tail to reduce the weight that would be increased and the area of the body that would result in drag. Also some edits in integral coefficient of Yaw and Roll control to have rapid correction during the first tests. That resulted in a drifted lagged response causing error in roll hence stall after a few meters of take-off. After laser cutting new materials and assembling a new tail and fuselage, a stable flight test successfully performed with a good seated PID roll/yaw coefficient in three flight tests.

Communication:

During this flight tests RC communication channel and telemetry channel with both 433Mhz and 915Mhz modules tested with good ranges and RSSI during the flight in a range of 320 meters.

High force movement:

- high climb angles of 25 and descent of -25 degree is tested in stabilize mode.
- high speed climb after descent is tested to ensure wing load strength, a quite more dihedral angle has shown, but no structure failure happened. as a test for a kamikaze mission.

Speeds:

Take off speed of around 13, like 12.53 calculated stall. max speed shown in long waypoint shown 34, but it could be increased with a higher propeller of 15x8. Also the distance between points is not long enough to reach the maximum velocity.

A lot of more tests of the UAV itself need to be done for stability and to stimulate the dog-fight and kamikaze mission. Then a controller tests and system tests.

9 SAFETY

We prioritize safety When building and testing UAVs. Risks that compromise security are evaluated based on their frequency of occurrence and consequences. We first identify potential threats, then evaluate their likely consequences if they occur, and finally, we estimate the likelihood that these threats will materialize. Risks are weighed against a set of approved criteria. The after-measures threshold is one. The hazards are analyzed and reassessed after the actions have been taken. Additional steps are performed if the amount remains above the threshold.

Department	Risk	Before Precaution		Precaution	After Precaution		Risk Level		Reduction Rate (%)	Responsible Person
		Likelihood (0-10)	Severity (0-10)		Likelihood (0-10)	Severity (0-10)	Before Precaution	After Precaution		
General	Work injury	3	8	Equipping a first aid kit	1	4	2.4	0.4	83	Salah
	wrong calculation	3	8	Using simulation software and real life testing	2	4	2.4	0.8	67	all the team
	Storms / Rain / Snow	2	8	Use airspeed meter to evaluate weather situation	2	4	2.4	2.8	67	Abdelbasit
Mechanical	Some parts are broken	5	9	Use spare parts	2	5	4.5	1	78	Baran
	wrong installation	4	7	One way installation way design applied	1	2	2.8	0.2	93	
Control, Avionics, and wiring.	Autonomous system failure	3	6	switch to rtl mode	1	5	1.8	0.5	72	Halid
	GPS system failure	5	4	switch to manual control	1	2	2	0.8	60	
	Manual control link failure	2	8	perform fail-safe maneuver	2	4	2.4	2.8	67	
	Motor or esc failure	3	9	emergency landing	1	2	2.7	0.2	93	
	battery explosion	3	9	Well Packing	1	2	2.7	0.2	93	
	Wrong wiring	3	9	Use checklist before flying	1	9	2.7	0.9	67	
	drone collision	3	9	Use spare parts	1	2	2.7	0.2	93	
	Improper mission-plan	5	4	Use data Correction from control server	2	4	2	0.8	60	
	Battery out of charge	6	7	Use battery level tester	3	3	4.2	0.9	79	
	Exit the flight zone	3	6	Use manual control	1	4	1.8	0.4	78	
Communication	Signal interference & traffic	3	6	Change control channel	1	5	1.8	0.5	72	Omar
	Telemetry lose	4	7	Troubleshooting control system	1	2	2.8	0.2	93	
	Connection out of range	3	6	Use manual control	1	4	1.8	0.4	78	
Software	Critical software error	3	9	Troubleshooting software	1	9	2.7	0.9	67	Ahmed

Table 7: Risks assessment

References

- [1] Ardupilot documentation. (n.d.). Retrieved from <https://ardupilot.org/plane/index.html>
- [2] Beard, R. W., & McLain, T. W. (2012). *Small unmanned aircraft: Theory and practice*. Princeton University Press.
- [3] MAVLINK Common Message Set. MAVLink Developer Guide. (n.d.). Retrieved from <https://mavlink.io/en/messages/common.html>
- [4] Nvidia Jetson Developer Tools. NVIDIA Developer. (2019, July 30). Retrieved from <https://developer.nvidia.com/embedded/develop/>
- [5] OpenCV modules. OpenCV. (n.d.). Retrieved from <https://docs.opencv.org/4.x/>
- [6] PX4 autopilot user guide (master). PX4 User Guide. (n.d.). Retrieved from <https://docs.px4.io/master/en/>
- [7] Python API reference. DroneKit. (n.d.). Retrieved from <https://dronekit-python.readthedocs.io/en/latest/automodule.html>
- [8] Raymer, D. P. (1992). *Aircraft design:A conceptual approach*.
- [9] Ultralytics. (n.d.). Yolov5 . GitHub. Retrieved from <https://github.com/ultralytics/yolov5>